Sensory cutaneous papillae in the sea lamprey (Petromyzon marinus L.):
I. Neuroanatomy and physiology.

SCHOLARONE™
Manuscripts

1   Sensory cutaneous papillae in the sea lamprey (*Petromyzon marinus* L.):

2   I. Neuroanatomy and physiology.

3

4   Short Title: Cutaneous papillae in Lampreys

5

6   Gheylen Daghfous[1,2], François Auclair[1], Felix Blumenthal[1], Tina Suntres[3], Jessica Lamarre-

7   Bourret[1], Masoud Mansouri[1], Barbara Zielinski[3,4] and Réjean Dubuc[1,2,*]

8

9   [1] Groupe de Recherche sur le Système Nerveux Central, Département de neurosciences,

10   Université de Montréal, Montréal, QC, Canada

11   [2] Groupe de Recherche en Activité Physique Adaptée, Département des sciences de l'activité

12   physique, Université du Québec à Montréal, Montréal, QC, Canada

13   [3] Department of Biological Sciences, University of Windsor, Windsor, ON, Canada

14   [4] Great Lakes Institute for Environmental Research, University of Windsor, Windsor, ON, Canada

15

16

17

18

19

20   *Correspondence: Réjean Dubuc, Ph.D., Professor, Département des sciences de l'activité

21   physique, Université du Québec à Montréal, PO Box 8888, section Centre-ville, Montréal,

22   Québec, H3C 3P8, Canada.

23   rejean.dubuc@gmail.com

1

Acknowledgments

Conflict of Interest Statement

The authors wish to declare no conflict of interest.

Data Availability Statement

The data that support the findings of this study are available from the corresponding author upon reasonable request.

Abstract

2

47   Molecules present in an animal's environment can indicate the presence of predators, food or

48   sexual partners and consequently, induce migratory, reproductive, foraging, or escape behaviors.

49   Three sensory systems, the olfactory, gustatory, and solitary chemosensory cell (SCC) systems

50   detect chemical stimuli in vertebrates. While a great deal of research has focused on the olfactory

51   and gustatory system over the years, it is only recently that significant attention has been devoted

52   to the SCC system. The SCCs are microvillous cells that were first discovered on the skin of fish,

53   and later in amphibians, reptiles, and mammals. Lampreys also possess SCCs that are particularly

54   numerous on cutaneous papillae. However, little is known regarding their precise distribution,

55   innervation, and function. Here, we show that sea lampreys (*Petromyzon marinus* L.) have

56   cutaneous papillae located around the oral disc, nostril, gill pores, and on the dorsal fins and that

57   SCCs are particularly numerous on these papillae. Tract-tracing experiments demonstrated that

58   the oral and nasal papillae are innervated by the trigeminal nerve, the gill pore papillae are

59   innervated by branchial nerves, and the dorsal fin papillae are innervated by spinal nerves. We

60   also characterized the response profile of gill pore papillae to some chemicals and showed that

61   trout-derived chemicals, amino acids, and a bile acid produced potent responses. Together with

62   a companion study, (Suntres, Daghfous, Dubuc, & Zielinski, this issue), our results provide new

63   insights on the function and evolution of the SCC system in vertebrates.

64

65

66   Keywords

70

71

1. Introduction

73 Chemoreception is not restricted to olfaction and gustation (Daghfous, Green, Zielinski, & Dubuc,

74 2012; Finger, 1997; Hansen & Reutter, 2004; Kotrschal, 1996; Parker, 1912). Chemicals that are

75 present in the environment are also detected by specialized epithelial cells named "solitary

76 chemosensory cells" (SCCs). Bipolar epidermal cells thought to be sensory were initially described

77 in lampreys (Fahrenholz, 1936a, 1936b; Foettinger, 1876; Langerhans, 1873) and in ranid tadpoles

78 (Kölliker, 1885; 1886). However, it is only with the work of Whitear on the skin of teleost fish that

79 the innervation, and thus sensory nature, of these cells was demonstrated (Lane & Whitear, 1982;

80 Whitear, 1952, 1965, 1971). Subsequently, studies have reported putative SCCs on the barbels

81 and nasopharynx of hagfish (Braun, 1996; 1998; Braun & Northcutt, 1998), on the skin surface of

82 brook lampreys (*Lampetra planeri* Bloch) and river lampreys (*Lampetra fluviatilis* L.), including the

83 oral, gill pore, dorsal fin and genital regions (Baatrup & Døving, 1985; Fox, Lane, & Whitear, 1980;

84 Whitear & Lane, 1983a), on the skin, gills, and oropharynx of chondrichthyes and bony fish (Codina

85 et al., 2012; Hansen, Ghosal, Caprio, Claus, & Sorensen, 2014; Kotrschal, 1992; Kotrschal,

86 Krautgartner, & Hansen, 1997; Kotrschal, Peters, & Atema, 1989; Kotrschal, Whitear, & Adam,

87 1984, Kuciel et al., 2014; Peach, 2005; Peters, Kotrschal, & Krautgartner, 1991; Peters, Van

88 Steenderen, & Kotrschal, 1987; Silver & Finger, 1984; Whitear & Moate, 1994). Other studies have

89 described solitary chemosensory cells on the skin and in the oral cavity of amphibians (Koyama,

90 Nagai, Takeuchi, & Hillyard, 2001; Nagai, Koyama, Von Seckendorff Hoff, & Hillyard, 1999; Osculati

91 & Sbarbati, 1995; Whitear, 1976), and in the airways of reptiles and mammals (Finger et al., 2003;

92 Hansen, 2007; Saunders, Christensen, Finger, & Tizzano, 2014; Sbarbati, Crescimanno, Benati, &

93 Osculati, 1998; Sbarbati, Crescimanno, Bernardi, & Osculati, 1999; Sbarbati & Osculati, 2003;

94 Tizzano, Merigo, & Sbarbati, 2006; Tizzano et al., 2010). The study of SCC innervation and

4

95   physiology has been challenging because of the scarcity and widespread distribution of these

96   cells. Until recently, most knowledge regarding SCC innervation came from two teleost taxa: sea

97   robins (*Prionotus carolinus*) and rocklings (genera *Ciliata* and *Gaidropsarus*). In sea robins, SCCs

98   are concentrated on the free rays of the pectoral fins, and are innervated by spinal nerves

99   (Bardach & Case, 1965; Finger, 1982, 2000; Kotrschal, 1995; Morril, 1895). In rocklings, SCCs are

100   concentrated on the anterior dorsal fin and are innervated by a recurrent branch of the facial

101   nerve (Kotrschal, 1991, Kotrschal et al., 1984; Kotrschal, Royer, & Kinnamon, 1998; Kotrschal &

102   Whitear, 1988; Kotrschal, Whitear, & Finger, 1993b; Whitear & Kotrschal, 1988). More recent

103   studies have shown that the trigeminal nerve provides innervation to some of the SCCs located in

104   the distal nasal cavity of mammals and reptiles (Finger et al., 2003; Hansen, 2007; Tizzano et al.,

105   2010). Information regarding the physiology and function of the SCCs is also limited. In sea robins,

106   SCCs detect amino acids, which act as feeding cues and promote foraging in this species (Bardach

107   & Case, 1965; Silver & Finger, 1984), whereas SCCs respond to fish mucus in rocklings (Peters et

108   al., 1991, 1987) and brook lampreys (Baatrup & Døving, 1985). In rocklings, SCCs are narrowly-

109   tuned to mucus from heterospecific fish and likely act as a predator-detection system (Kotrschal,

110   Peters, & Atema, 1993; Peters et al., 1991, 1987). Their function in brook lampreys is not clear. In

111   mammals, airway SCCs respond to bacterial signals (Tizzano et al., 2010). Their activation evokes

112   respiratory protective reflexes (i.e. coughing and sneezing) through the activation of trigeminal

113   fibers (Finger et al., 2003) and stimulates the secretion of antimicrobial peptides (Lee et al., 2014,

114   2017). SCC locations, innervation patterns, and functions thus differ greatly in the few species that

115   have been studied and the solitary chemosensory cell system may be highly specialized in these

116   species (Finger, 1997). While these studies have been informative with regards to SCCs in given

117   vertebrate taxa, the general role of this chemosensory system is still unknown.

5

118   The present study examines SCC localization, chemical sensitivity, and innervation in the

119   sea lamprey (*Petromyzon marinus* L.). A companion study, (Suntres et al., this issue), investigates

120   the biochemical properties and development of SCCs during the life cycle of the sea lamprey.

121   Together, these two studies advance our understanding of the solitary chemosensory system in

122   the most basal extant vertebrate group. Knowledge on the SCC system in lampreys is crucial to

123   bridge the gap between studies conducted in fish and mammals. Due to the basal phylogenetic

124   position of lampreys within vertebrates, this research sheds light on the general organization and

125   role of the SCC system in vertebrates.

126

127

128   2. Materials and Methods

129   **2.1 Animals**

130   Experiments were performed on 54 spawning phase adults and 6 newly-transformed sea

131   lampreys (*Petromyzon marinus*) of both sexes. Animals were collected from the Pike River

132   (Québec, Canada). Agents of the U.S. Fish and Wildlife Service (Vermont and Michigan, USA) and

133   the Department of Fisheries and Oceans (Sault Ste. Marie, Canada) provided us with the spawning

134   adults. The animals were kept in aerated fresh water maintained at 4-5°C. All surgical and

135   experimental procedures conformed to the guidelines of the Canadian Council on Animal Care

136   (CCAC) and of the animal care and use committee of the Université de Montréal, the Université

137   du Québec à Montréal, and the University of Windsor.

138

139   **2.2 Anatomy and scanning electron microscopy (SEM)**

140   Since cutaneous papillae contain a high density of SCCs in brook and silver lampreys (Baatrup &

141   Døving, 1985; Fox et al., 1980; Whitear & Lane, 1983a), the distribution of cutaneous papillae was

6

142   established in the sea lampreys by carefully examining the body surface of larval, newly

143   transformed, parasitic and spawning animals under a stereomicroscope. This examination was

144   either performed directly on live, anesthetized animals or on fixed tissue samples. Live specimens

145   were anesthetized using tricaine methanesulphonate (MS-222, 100 mg/l, E10521, Sigma-Aldrich

146   Canada, Oakville, ON, Canada) and placed in a water-filled dish under a Nikon SMZ800

147   stereomicroscope (Nikon Canada, Mississauga, ON, Canada). Tissue samples were collected from

148   deeply-anesthetized   animals   (MS-222,   200   mg/l)   and   quickly   transferred   into   4%

149   paraformaldehyde (PFA, O4042-500, Fisher Scientific Canada, Ottawa, ON, Canada) dissolved in

150   phosphate buffered saline (PBS, 0.1 M, NaCl 0.9%, pH 7.4) and stored at 4°C. Fixed tissue samples

151   were examined and photographed with a Carl Zeiss Discovery V20 stereoscope fitted with an

152   AxioCam HRc camera running on Zen Digital Imaging for Light Microscopy Software V1.1.1.0 (Carl

153   Zeiss Canada, Toronto, ON, Canada, RRID:SCR_013672). Cutaneous papillae were counted on

154   fixed tissue samples under a stereomicroscope using an insect pin mounted on the tip of a Pasteur

155   pipette. For scanning electron microscopy, skin tissue samples were collected from the oral, nasal,

156   gill pore, and dorsal fin regions of deeply-anesthetized lampreys then quickly transferred into a

157   5% glutaraldehyde in 0.1 M sodium cacodylate fixative solution for at least 18 hours, rinsed in

158   0.1M sodium cacodylate buffer, and post fixed for 2 h in 2% osmium tetroxide in 0.1M sodium

159   cacodylate buffer. The skin samples were then dehydrated in an ethanol series of increasing

160   concentration, critical point-dried, and gold sputter-coated (Integrated Microscopy Biotron

161   Facility, Western University) before observation on a FEI Quanta 200 FEG SEM microscope (Great

162   Lakes Institute for Environmental Research, University of Windsor). Biometrics (length and width)

163   of cutaneous papillae were derived from low magnification electronmicrographs (SEMs).

164

165   **2.3 Injection of neuroanatomical tracers into cutaneous papillae**

166   For *in vivo* injections of papillae, anesthetized animals were laid down on their side in a dish and

167   kept moist by perfusing the dish with fish tank water. The papillae to be injected (only one type

168   per animal) were cut with fine scissors (McPherson-Vannas Scissors, 8cm, curved, 5mm blades,

169   #501234, World Precision Instruments, Sarasota, FL, USA) under a stereomicroscope and the

170   stumps were immediately covered with large crystals of biocytin (B-4261, Sigma-Aldrich Canada)

171   for 10-15 min. The injected papillae were then thoroughly rinsed with water. The animal was

172   transferred into an isolated fish tank until it recovered completely from anesthesia (around 60

173   min); it was then returned into a regular fish tank for 1 to 2 weeks to allow for axonal transport

174   of the tracer. At the end of this period, the animal was deeply anesthetized and decapitated

175   caudal to the 7th gill pore. The head was transferred into cold (8–10°C), oxygenated Ringer's (in

176   mM: 130 NaCl, 2.1 KCl, 2.6 CaCl2, 1.8 MgCl2, 4.0 HEPES, 4.0 dextrose, and 1.0 NaHCO3, at pH 7.4).

177   All tissue around the cranium was removed and the brain was exposed dorsally. For dorsal fin

178   papillae injections, a 5 cm-portion of the whole body (3 cm rostral and 2 cm caudal to the injection

179   site) was additionally collected and transferred into cold oxygenated Ringer's, where the tissue

180   ventral to the notochord was removed. After axonal transport of the tracer, the collected tissue

181   was fixed in PFA for 24 h at 4°C and processed for biocytin histochemistry as described below.

182

183   **2.4 Taste bud or cranial nerve injections**

184   Injections of pharyngeal taste buds and whole nerve (nV or nIX/X) were carried out on semi-intact

185   preparations of newly-transformed lampreys. The animal was deeply anesthetized and

186   decapitated caudal to the heart before being transferred into Ringer's. With the heart pumping,

187   the blood in the preparation was gradually replaced by cold, oxygenated Ringer's solution.

188   Meanwhile, the brain was rapidly exposed dorsally, and decerebration achieved with a complete

Journal of Comparative Neurology

189   transverse section just rostral to the mesencephalon. As the preparation recovered from

190   anesthesia, the gills began contracting again and followed a normal breathing rhythm.

191   The following protocol was used for nerve injections, to label their peripheral portion towards the

192   papillae (nV, n = 1; nIX/X, n = 1) or their central projections (nIX/X, n = 2). The nerves were cut

193   unilaterally at their exit from the brainstem and crystals of biocytin were applied between the

194   proximal and distal stumps of the cut nerves for 10-15 min. After thorough rinsing, the

195   preparation was transferred into a cooled chamber filled with 500 ml of re-circulated, oxygenated

196   Ringer's for tracer transport overnight. The next day, the preparation was fixed with cooled PFA,

197   post-fixed for 24 h at 4°C, and processed for the visualization of biocytin (see below).

198   For taste bud injections (n = 2), the preparation was further dissected by making a midline incision

199   of the ventral surface of the animal to gain access to the caudal part of the pharynx (sometimes

200   referred to as respiratory tube or as water tube), where the internal gill pores of the gill baskets

201   open and where the taste buds lie. Two or three taste buds caudal to the first and second internal

202   gill pores on one side were delicately disrupted with the pointed end of a pulled glass micropipette

203   to cut some of their innervating axons. Crystals of biocytin were immediately deposited on the

204   taste buds and left there to dissolve for 10-15 min. The taste buds were then rinsed thoroughly

205   and the preparation was transferred into a cooled chamber filled with Ringer's, for tracer

206   transport overnight as described above. The next day, the central nervous system was dissected

207   out and fixed by immersion in PFA for 24 h at 4°C and processed for the visualization of biocytin

208   (see below).

209

210   **2.5 Histology and histochemistry**

211   Samples (skin tissue, whole heads, or isolated central nervous system preparations) were

212   transferred from PFA to a solution of 20% sucrose in phosphate buffer. Samples were

9

213   subsequently frozen by immersion in 2-methylbutane (O-3551, Fisher Scientific Canada) at -45°C.

214   The preparations were embedded in Tissue-Tek OCT (#4583, Sakura Fineteck, Torrance, CA, USA;

215   diluted 1:10 with dH$_2$O), and 25 µm-thick transverse sections were cut on a cryostat (Cryo-Cut

216   microtome, Model 845, AO Instrument Co., Buffalo, NY, USA). The sections were collected on

217   ColorFrost Plus microscope slides (Fisher Scientific, Canada) and air-dried overnight on a warming

218   plate set at 37°C. The following day, the tissue sections were rinsed 3 times 10 min with PBS and

219   then incubated for 120 min in PBS containing 0.3% Triton and one or two of the following:

220   streptavidin conjugated to Alexa Fluor 594 or 488 (Thermo Fisher Scientific Cat# S-11227,

221   RRID:AB_2313574, lot 1704463 and Cat# S11223, RRID:AB_2336881, lot 1694695; dilution 1:400,

222   Molecular Probes, Eugene, OR, USA) and/or phalloidin conjugated to Alexa Fluor 488 (Molecular

223   Probes Cat# A-12379, RRID:AB_2315147, lot: 1859640, dilution 1:100, Molecular Probes). The

224   sections were then rinsed 3 times 10 min with PBS and mounted with Vectashield with or without

225   DAPI (H-1000 or H-1200, Vector laboratories, Burlington, ON, Canada) or processed for

226   fluorescent Nissl staining with Neurotrace Green (120-minute incubation, diluted 1:200 in PBS at

227   room temperature) before mounting. The sections were then observed under epifluorescence

228   microscopy and photographed with an E600 microscope equipped with a DXM1200 digital camera

229   (Nikon Canada). The diameter of axons was measured with an intraocular microscale directly

230   under the microscope.

231

232   **2.6 Electrophysiological recordings and chemical applications**

233   Electrophysiological experiments were performed on *in vitro* isolated skin preparations pinned

234   down to the bottom of a recording chamber lined with Sylgard (Dow Corning, Midland, MI) and

235   continuously perfused with cold oxygenated Ringer's (~4 ml/min, total volume of chamber = 50

236   ml). Glass electrodes (Ø±50 µm) filled with Ringer's solution were placed over the tip of one

237   papilla under visual guidance through a Wild M3C stereomicroscope (Wild, Heerbrugg,

238   Switzerland) to record multiunit activity. The signals were amplified (x10k) and filtered (100Hz-

239   1kHz band-pass) using an AM systems 1800 dual channel amplifier (AM systems Inc, Everett, WA)

240   and digitized using a Digidata 1322A interface running on Clampex V9.2 software (Axon

241   Instruments, Molecular Devices, Union City, CA, USA, RRID:SCR_011323). Chemical stimulation

242   was delivered through a small plastic tube (Ø±500 µm) positioned over the recorded papillae

243   connected to a 6-port injection valve (V-450, Upchurch Scientific, Oak Harbor, WA, USA). Test

244   solutions were loaded into the 100 µL sample loop of the injection valve and inserted into a

245   continuous flow (~4ml/min) of Ringer's solution to avoid pressure variations. With this method,

246   delivery of the chemicals occurred over a period of approximatively 30 s. The test solutions were

247   delivered in a random order with a 5 min inter-stimulus interval, with three consecutive

248   applications for each stimulus. In other experiments, chemical stimulation was delivered through

249   a glass micropipette connected to a pressure ejection system (4s train, 4 Hz, 20 ms pulse duration,

250   ~4 psi, Picospritzer, General Valve, Fairfield, NJ). The inert dye Fast Green FCF (F99-10, Fisher

251   Scientific, Canada) was added to the solutions to monitor the delivery of the test solution to the

252   recorded papilla. Amino acids used in this study were all L-forms. All chemical substances tested

253   were diluted in Ringer's and applied at 10^{-3} M except for the thawed trout water (unknown

254   concentration, referred to as "trout water" hereafter) and lamprey sex pheromones (3-keto-

255   petromyzonol sulfate or 3kPZS, 10^{-5} M; 3-keto-allocholic acid or 3kACA; 10^{-5} M). The pH of these

256   solutions ranged from 6.9 to 7.4. Ejections of Ringer's solution were used as a blank control in

257   each experiment. All chemicals except the pheromones and trout water were purchased from

258   Sigma-Aldrich Canada. Pheromones were a courtesy of Dr. Weiming Li (Michigan State University,

259   MI). Trout water was prepared by thawing a frozen rainbow trout in Ringer's and filtering the

260   resulting solution (adapted from Baatrup & Døving 1985). Chemicals were kept as frozen

11

261   concentrated stock solutions and dissolved to their final concentration in Ringer's solution prior

262   to their use.

263

264   **2.7 Data analysis and statistics**

265   Electrophysiological signals were analyzed using Spike2 V5.19 (Cambridge Electronic Design,

266   Cambridge, UK, RRID:SCR_000903) and Clampfit V10.5 (pClamp, Molecular Devices, Union City,

267   CA, USA, RRID:SCR_011323,) software. Signal offsets were set to zero prior to any analysis.

268   Discharges were detected using an amplitude threshold set as five times the standard deviation

269   of the signal in control condition (Pouzat, Mazor, & Laurent, 2002). Raster plots and associated

270   peristimulus time histograms (PSTHs) were generated for each series of three consecutive

271   applications of a given chemical stimulus. PSTHs were computed over a period of 180 s with a bin

272   width of 1 s. The first 30 s served as the control period followed by 30 s of stimulation, and 120 s

273   post stimulus. The last 30 s of the post stimulus period were considered as the washout period.

274   The mean discharge frequency of each series of three applications over the control, stimulation,

275   and washout periods were compared using one-way repeated measures analysis of variance

276   followed by Holm-Sidak's multiple-comparison post-hoc test or Friedman repeated measures

277   analysis of variance on ranks followed by Tukey's multiple-comparison post-hoc test. Significant

278   changes in mean discharge frequency during control and chemical application were considered

279   as responses. An increase in mean discharge frequencies was classified as an excitatory response,

280   whereas a decrease was considered as an inhibitory response. Results are presented as mean ±

281   SD. Statistical analyses were performed using Sigma Plot V11.0 (Systat Software, San Jose, CA,

282   USA, RRID:SCR_003210). Statistical significance was set at $p < 0.05$. The majority of

283   photomicrographs and SEMs were adjusted for brightness and contrast, and the ones illustrating

284   phalloidin labeling of microvilli were also sharpened slightly, all using Photoshop software CS5

12

285   (Adobe Systems, San Jose, CA, USA, RRID:SCR_014199). Drawings and figure assembly was carried

286   out using Illustrator software CS5 (Adobe Systems, San Jose, CA, USA, RRID:SCR_010279).

287

288

289   3. Results

290   **3.1 Location of cutaneous papillae**

291   Newly-transformed lampreys had small papillae, which became more prominent during parasitic

292   stage, and reached full development in spawning stage. Therefore, the present investigation

293   focused on the spawning adults (for a detailed account of papillae development see *Suntres et al.*

294   in this issue). In spawning adult *P. marinus*, cutaneous papillae were found around the oral disc

295   (N = 25.6 ± 4.8), on the skin bordering the nostril (N = 16.6 ± 2.5), on the posterior margin of each

296   gill pore (N = 38.5 ± 6.7), and on the trailing edges of the dorsal fins (anterior: N = 329.3 ± 62.7;

297   posterior: N = 669.7 ± 166.0) (Fig. 1 and Table 1). Despite a generally similar form, the papillae

298   displayed some variations in size and shape at the different locations (Table 2).

299

300   **3.2 Microvilli-bearing cells on oral, nasal, gill pore, and dorsal fin papillae**

301   Tufts of microvilli emerged at the junction between the epidermal cells covering the

302   surface of oral, nasal, gill pore, and dorsal fin papillae viewed by SEM (Fig. 2). Tissue sections

303   labeled for F-actin with fluorescent phalloidin, showed that the microvilli extended from narrow

304   epidermal cells present in oral (n = 5), nasal (n = 7), gill pore (n = 5), and dorsal fin (n = 8) papillae

305   (Fig. 3a1,b1,c1,d1). Oral and gill pore papillae had the highest concentration of microvillar tufts in

306   both SEM (Fig. 2a1 and 2c1) and phalloidin labeled preparations (Fig. 3a1 and 3c1). Tufts of

307   microvilli were sparser on dorsal fin papillae (Fig. 3d1) and only a few were seen on the surface of

308   nasal papillae (Fig. 3b1). Phalloidin labeling was used to examine the morphology of the

13

309   microvillar cells. On sections, phalloidin labeled the actin core of microvilli intensely, slightly more

310   in the protruded portion of the microvilli than in the non-protruded portion, and it also labeled

311   the cell membrane of all cells in the papillae. Most of the microvilli-bearing cells had an elongated

312   piriform shape typical of SCCs (Fig. 3, magenta arrows) and they each bore many microvilli at their

313   apex, regardless of the type of papilla. The detailed microvillar organization was not examined

314   here, but SCCs on gill pore papillae appeared to bear the longest microvilli (Fig. 3c, all 12

315   photomicrographs in columns 2 to 4, including the inset in (b2), are at the same magnification).

316   In some animals, microvilli seemed absent from the surface of papillae, regardless of their location

317   on the body. In those cases, phalloidin only labeled cell apices without obvious protrusions. The

318   reasons for these differences are not clear.

319   In addition to SCCs, phalloidin also labeled Merkel cells (Fig. 3, arrowheads) as they bear

320   microvilli with a F-actin core at opposite poles of their cell body (Whitear & Lane, 1981). All

321   papillae investigated in our study contained Merkel cells. Dorsal fin and nasal papillae had a typical

322   aggregation of these cells at their tip (Figs. 3b2, inset, and 3d4 illustrate examples). Oral papillae

323   contained numerous Merkel cells spread out evenly in their epithelium, some located

324   superficially, and others deeper in the epithelium (Fig. 3a3-4), reminiscent of the epithelium

325   elsewhere on the body. A few Merkel cells were also seen on almost every gill pore papilla (Fig.

326   3c4 shows an example).

327   Our investigation of oral papillae also showed that fimbriae (n = 3, whole; n = 2 on

328   sections; see Fig. 1b), which are flat skin extensions with digit-like protrusions at their tip located

329   immediately behind the papillae,   had numerous microvilli on their surface, in a manner

330   reminiscent of the oral papillae. On sections, the fimbriae also contained numerous Merkel cells,

331   like oral papillae.

332

14

3.3 Papillae respond to chemical stimulation

Responses to chemical stimulation were primarily investigated on gill pore papillae because they showed, like oral papillae, the largest concentration of SCCs and the lowest number of Merkel cells (see Fig. 3). The initial placement of the recording electrode over the papillae (Fig. 4, Top) generally produced a few discharges that subsided within a minute. A basal activity of the papillae in the absence of chemical stimuli was present in most of the animals examined (n = 13). Within one trial, 5-10 units were generally observed in the recording. The analysis was, however, not performed on individual units (see materials and methods section for more details). Chemical application over the papillae typically induced excitatory responses (i.e. a significant increase in mean discharge frequency). However, in limited cases (4 trials in 2 animals), it produced a significant decrease in mean discharge frequency (i.e. inhibitory responses). Figure 4 shows examples of responses to different chemicals and Table 3 shows trial statistics. Trout water repeatedly produced strong responses; it elicited excitatory responses in all but two animals (11/13). The amino acids, glycine and proline, elicited excitatory responses in more than half of the animals (7/12). Taurocholic acid, a bile acid, elicited excitatory responses in a little less than half of the animals (5/13) and sialic acid, a mucus component, elicited responses in about one third of the animals (3/10). Responses to the other amino acids tested (serine, glutamate, arginine, histidine) were less frequent and sex pheromones (3kPZS, 3kACA) did not induce any responses (Table 3). Serine, glutamate and arginine produced a few inhibitory responses. Our data did not reveal any clear clustering of gill pore papillae based on their response profile to the different chemical stimuli. The precise response profile of the other types of papillae (oral, nasal, and fin) was not investigated here, but their chemosensory function was ascertained by puffing trout water using a pressure ejection system over the papillae in a few animals (n = 4). In this series of experiments, we tested whether the papillae responded to mechanical stimuli by puffing

15

357   jets of Ringer's over the papillae. Gill pore papillae did not show responses, whereas mechanical

358   stimulation of oral, nasal or fin papillae sometimes produced discharges. When seen, short

359   duration bursts of only a few seconds (unlike responses to chemical stimulation) always

360   characterized the responses to mechanical stimulation of the papillae.

361

362   **3.4 Innervation of papillae by ganglion cells and their central projections**

363   The four types of papillae investigated were all innervated by peripheral, bipolar ganglion

364   cells, never by dorsal cells within the central nervous system. Injections of tracer in oral papillae

365   of spawning adult lampreys (n = 2) labeled ganglion cells in the maxillomandibular part of the

366   trigeminal ganglion, while tracer injections in the nasal papillae of spawning adult lampreys (n =

367   2) labeled ganglion cells in the ophthalmicus profundus part of the trigeminal ganglion (Fig. 5).

368   For oral and nasal papillae, the central processes of the ganglion cells were coarse (3-4 µm). In

369   both cases, they entered the brainstem through the trigeminal sensory root (Fig. 5a1,a2) to join

370   the descending root of the trigeminal nerve (rdV) and reach the first spinal segment. Our

371   investigation did not include more caudal levels of the spinal cord. Injections (n = 2) of the cut

372   distal end of the trigeminal sensory nerve at its exit from the cranium labeled fibers that entered

373   the nasal and oral papillae (Fig. 6a,c). These injections also labeled fibers innervating the fimbriae

374   around the oral disc (Fig. 6b).

375   Axonal tracing experiments focused on papillae from gill pores 1 to 3 of spawning adult

376   lampreys (n = 6). Injections of tracer in papillae located at the first gill pore labeled cells in the

377   glossopharyngeal ganglion, while tracing from gill pore papillae located at the second and third

378   gill pores labeled cells in close relation to the main trunk of the vagus nerve. Occasional ganglion

379   cells were seen along the vagus nerve root innervating a gill, although not a great distance from

380   the main trunk of the vagus nerve. Their labeled central processes were coarse (around 4 µm) and

16

381   entered the brainstem through the glossopharyngeal nerve (first gill pore injections) or through

382   one of the roots of the vagus nerve (second and third gill pore injections). Upon entering the

383   brainstem, they immediately coursed towards a more dorso-medial position in the alar plate to

384   join a longitudinal tract (Fig. 7b1, white arrows). Most of them turned caudally in that tract (Fig.

385   7c1) to reach at least the first spinal segment. A small number of the entering axons joined the

386   same tract but coursed rostrally (Fig. 7a1). We could not determine in our material if these were

387   different axons or branches of some of the descending axons. Injections of the cut distal end of

388   the glossopharyngeal and vagus nerve at their exit from the cranium, labeled fibers that entered

389   the gill pore papillae (Fig. 6d, n = 2).

390   The central projections from gill pore papillae constitute only a portion of all the afferents

391   entering the brainstem by cranial nerves IX and X, as shown by the comparison to injections of

392   whole nerves IX and X (see Fig. 7a3-c3, injections of nIX and nX, n = 3). To compare their central

393   projections with those from taste buds, whose afferents are known to enter the brainstem

394   through cranial nerves VII, IX and X in many vertebrates (Finger, 1997), we injected taste buds in

395   the pharynx of newly-transformed animals (n = 2). These injections produced a labeling pattern

396   that differed from that obtained after gill pore papillae injections. First, the fibers innervating the

397   taste buds were of finer caliber (around 2 µm) and formed a longitudinal tract immediately after

398   entering the brainstem, at the lateral edge of the alar plate (Fig. 7b2). More fibers seemed to turn

399   caudally than rostrally in that tract, although the rostral projection was significant. From the point

400   of entrance of nIX to the level of the obex, fine varicose fibers left the longitudinal tract in a medio-

401   dorsal direction to terminate in a well-delineated nucleus, just adjacent to the tract, in the lateral

402   alar plate. This nucleus has been previously suggested to be the lamprey homologue of the

403   mammalian nucleus of the solitary tract (NTS), based on its location and neurochemical evidences

404   (Albersheim-Carter et al., 2016; Auclair, Lund, & Dubuc, 2004; Barreiro-Iglesias, Anadón, &

17

405   Rodicio, 2010; Pombal, López, de Arriba, González, & Megías, 2008; Pombal, López, de Arriba,

406   Megías, & González, 2006). The present data corroborate this homology hypothesis (see

407   Discussion). The ascending fibers coursed between the rdV and the vestibular area and

408   terminated at isthmic levels, just medial to the anterior octavomotor nucleus. The descending

409   fibers reached the level of the obex but did not seem to continue down to the spinal cord.

410   Injections of the cut distal end of the glossopharyngeal and vagus nerve at their exit from the

411   cranium, labeled fibers that innervated pharyngeal taste buds (Fig. 6e, n = 2). In one animal, the

412   skin dorsal to the 2nd and 3rd gill pores was carefully injected, making sure to spare neuromasts

413   in that area. The injection included the epidermis, dermis and the surface of the muscle layer. It

414   labeled ganglion cells close to the main trunk of the vagus nerve, but their central projections

415   entered the brainstem through the posterior lateral line nerve to terminate in the medial nucleus

416   of the octavolateral area. Other fibers travelling in the trunk lateral line nerve entered the

417   recurrent nerve. These fibers originated from ganglion cells located both in the intracapsular

418   ganglion and in the lateral portion of the anterior lateral line ganglion (see Koyama, Kishida, Goris,

419   & Kusunoki, 1990), and had central projections that terminated in the dorsal nucleus of the

420   octavolateral area. The skin injection also labeled spinal ganglion cells and dorsal cells within the

421   spinal cord, and ascending fibers were seen in the dorsal columns. These skin injections did not

422   label fibers resembling the ones that entered the brainstem through the vagus nerve after gill

423   pore papillae injections.

424   Tracer injections in 8 - 12 consecutive dorsal fin papillae of spawning adult lampreys (n =

425   3) labeled spinal ganglion cells on both sides of the animals. These cells were found either in the

426   dorsal root ganglions outside the spinal canal (Fig. 8a,b) or inside the spinal canal at different

427   levels along the dorsal roots (Fig. 8c,d). These injections never labeled dorsal cells (i.e. intraspinal

428   sensory ganglion cells) in our material. The ganglion cells innervating dorsal fin papillae were

18

429   bipolar with coarse axons (around 4 μm). The central processes from these cells entered the

430   dorsal spinal cord through the dorsal roots where they turned caudally and rostrally in the dorsal

431   funiculus. From the number of labeled ganglion cells and ascending and descending axons, it is

432   most probable that the entering axons gave rise to both an ascending and a descending branch,

433   although we could not see branching axons in our material. The individual descending branches

434   reached as far as 5 or 6 spinal segments more caudal than their own entrance point. Further

435   caudally, this translated into gradually fewer fibers in the dorsal funiculus until there were none

436   left. The ascending branches could be followed up to the last sections of our material (~ 3 cm

437   rostral to the injected dorsal fin papillae). Their numbers were similar to that of labeled ganglion

438   cells, which suggested that all ganglion cells projected at least this far rostrally. In 2 animals,

439   observations from sections of the brainstem failed to show labeled fibers from dorsal fin papillae

440   injections. The distance between the injected caudal dorsal fin and the brainstem was in the order

441   of 20 cm or so in these two animals, a distance that prevents efficient tract tracing in lampreys.

442   Contrary to the other types of papillae, we did not trace the fibers innervating dorsal fin papillae

443   from their exit from the spinal canal to the papillae.

444

445

4. Discussion

447   Despite recent advances (Finger et al., 2003; Hansen, 2007; Kirino, Parnes, Hansen,

448   Kiyohara, & Finger, 2013; Tizzano et al., 2006), information on the physiology and function of the

449   SCC system in vertebrates is limited. In this study, we established that SCCs are particularly

450   numerous on cutaneous papillae around the oral disc, nostril, gill pores, and on the dorsal fins in

451   the sea lamprey (*Petromyzon marinus*). We demonstrated that the oral and nasal papillae are

452   innervated by the trigeminal nerve, the gill pore papillae by the glossopharyngeal or vagus nerve,

19

453   and the dorsal fin papillae by spinal dorsal roots. We also characterized the chemical response

454   profile of gill pore papillae and showed that trout water and the amino acids, glycine and proline,

455   produced strong responses. A companion study, (Suntres et al., this issue), further investigates

456   the immunocytochemical properties and the development during ontogeny of the lamprey SCCs.

457   Together, these studies provide new insights on the function and evolution of the SCC system in

458   vertebrates.

459

460   **4.1 Location of cutaneous papillae and SCC distribution**

461   The first report of cutaneous papillae in lampreys long predates the discovery of SCCs.

462   Linnaeus (1758) described the mouth of *P. marinus* and *L. planeri* as "papilloſo". He wrote about

463   *L. planeri* : "Behind the border of the mouth are numerous sharp papillae" (as cited in Turton,

464   1803). Since then, other authors have reported the presence of papillae (oral - Baatrup & Døving,

465   1985; Cook, Hilliard, & Potter, 1990; Fox et al., 1980; Langerhans, 1873; Lethbridge & Potter, 1981;

466   Potter, Lanzing, & Strahan, 1968; Whitear & Lane, 1983a; Woodland, 1913; gill pore- Dawson,

467   1905; Whitear & Lane, 1983a; fin – Langerhans, 1873; Whitear & Lane, 1983a) and have assessed

468   the papillae as a taxonomic character (Beamish, 2010; Khidir & Renaud, 2003). However, these

469   studies did not look systematically at the morphology, anatomy, and physiology of the papillae.

470   Cells that are now recognized as SCCs were first mentioned by Langerhans (1873) who

471   described hair-bearing bipolar cells on the body surface that were particularly numerous on oral

472   papillae ("Mundpapillen") and dorsal fin papillae ("Flossenpapillen") in *L. planeri*. The cells

473   described by Langerhans and their possible innervation were re-examined and discussed by

474   anatomists in the late 19th - early 20th century (Fahrenholz, 1936a, 1936b; Ficalbi, 1914;

475   Foettinger, 1876; Fusari, 1907; Marenghi, 1903; Retzius, 1892; Studnička, 1913; Tretjakoff, 1927).

20

476   Electron microscopy allowed researchers to demonstrate the precise association of these cells

477   with nerve fibers in lampreys ("oligovillous cells", Fox et al., 1980; Whitear & Lane, 1983a).

478   Our investigation of SCCs in spawning phase *P. marinus* focused on papillae as they

479   contain a high density of SCCs in *L. planeri* and *L. fluviatilis* (Baatrup & Døving, 1985; Fox et al.,

480   1980; Whitear & Lane, 1983a). We confirmed previous reports (Dawson, 1905; Whitear & Lane,

481   1983a) describing a fringe of papillae close to the gill pores and of papillae around the oral disc

482   (Baatrup & Døving, 1985; Khidir & Renaud, 2003). The number of papillae at these two locations

483   (Table 1) is consistent with observations in other lamprey species (Beamish, 2010; Cook et al.,

484   1990; Khidir & Renaud, 2003). We also showed that *P. marinu*s bears papillae on the tip of the

485   dorsal fins, as described in *L. planeri* (Fox et al., 1980; Whitear & Lane, 1983a). Moreover, we

486   provide the first description of papillae on the edge of the nostril.

487   The epidermis covering the papillae located at the different locations was thinner and

488   simpler than elsewhere on the body. It contained occasional granular cells but no skein cells, as

489   reported by Lane and Whitear (1980) and Cook et al. (1990) (see also Rodríguez-Alonso, Megías,

490   Pombal, & Molist, 2017). Numerous cells with the typical elongated piriform shape of vertebrate

491   SCCs (Tizzano & Finger, 2013) and harbouring a tuft of microvilli-like extensions were seen. Our

492   anatomical experiments showed that these microvilli-like extensions contain a F-actin core,

493   confirming their microvillous nature. These cells correspond to the "oligovillous cells" of Fox et al.

494   (1980) and Whitear and Lane (1983a). They were later recognized as lamprey SCCs (Whitear,

495   1992) and our results support this hypothesis. We found particularly numerous SCCs on oral and

496   gill pore papillae, comparatively less on dorsal fin papillae, and only a few were observed on nasal

497   papillae. In addition to SCCs, papillae also contained Merkell cells. These cells bore microvilli at

498   opposite poles of their cell body, a typical feature of lamprey Merkel cells (Takahashi-Iwanaga &

499   Abe, 2001; Whitear, 1989; Whitear & Lane, 1981). Previous studies reported Merkel cells in oral

21

500   papillae in *L. planeri* (Baatrup & Døving, 1985) and *Geotria australis* (Cook et al., 1990). Our

501   material provided evidence of numerous Merkel cells on oral, nasal, and fin papillae, as well as a

502   few on gill pore papillae (often 1-2 per papilla) in *P. marinus*.

503   Although, we did not look for the presence of SCCs on the rest of the body, we examined

504   all the tissue that was collected around the papillae. From these observations, we found a large

505   number of SCCs with microvilli, similar to those of the oral papillae on the fimbriae surrounding

506   the oral disk. The external wall of the nostril contained a few SCCs that became rare on the

507   epidermis away from the nostril. The internal wall of the nostril leading to the olfactory epithelium

508   also contained SCCs, but their microvilli were different from that of the papillae SCCs. These cells

509   had only a few (3 to 5) straight microvilli, with a short protruded portion and a long non-protruded

510   portion. The microvilli in these SCCs formed an elongated narrow V shape. Similarly, Fox et al.

511   (1980) originally described two types of SCCs on the basis of the organization of the microvilli in

512   *L. planeri*. However, in a subsequent paper, the authors argued that they were more likely distinct

513   examples from a continuous series (Whitear & Lane, 1983a). Gill pore structures (i.e. ectal valve

514   and central process) occasionally contained SCCs , but rarely on the thicker epidermis around the

515   gill pores. The epidermis on of the dorsal fins also contained a few SCCs. In general, we did not

516   find many SCCs on the epidermis of the head and body, as reported previously by others on *L.*

517   *planeri* (Whitear & Lane, 1983a).

518   The SCC distribution is variable from one vertebrate species to the other. In aquatic

519   vertebrates, they are widely distributed on the skin, gills, nasopharynx, or oropharynx (hagfish -

520   Braun, 1996, 1998; Braun & Northcutt, 1998; lampreys - Baatrup & Døving, 1985; Fox et al., 1980;

521   Whitear & Lane, 1983a; chondrichthyes - Peach, 2005; Whitear & Moate, 1994; bony fish - Codina

522   et al., 2012; Hansen et al., 2014; Kotrschal, 1992; Kotrschal et al., 1997, 1989, 1984; Kuciel et al.,

523   2014; Peters et al., 1987, 1991; Silver & Finger, 1984; see Whitear, 1992 for a review). In terrestrial

524   vertebrates, on the other hand, SCCs seem restricted to specific anatomical locations (e.g. the

525   airways) (amphibians - Osculati & Sbarbati, 1995; Whitear, 1976; but see also for putative skin

526   SCCs Koyama et al., 2001; Nagai et al., 1999; reptiles - Hansen, 2007; mammals - Finger et al.,

527   2003; Saunders et al., 2014; Sbarbati et al., 1998, 1999; Sbarbati & Osculati, 2003; Tizzano et al.,

528   2010, 2006).

529   Chemical response profile and behavioral functionIn the present study, we have

530   examined the responses of papillae to chemicals that could potentially activate SCCs. We have

531   limited our study to chemicals that are known to activate chemosensory systems in lampreys. We

532   did not test all chemicals known to activate these systems in other species. Moreover, the

533   physiological experiments were limited to the responses of papillae in the gill region

534   We showed that gill pore papillae of sea lampreys respond strongly to trout water, to the

535   amino acids proline and glycine, and to the bile acid, taurocholic acid. Serine, sialic acid, and

536   glutamate also produced occasional excitatory responses. These results partially corroborate

537   those of Baatrup & Døving (1985) who electrophysiologically recorded from SCCs located around

538   the oral disc in *L. planeri*. They found responses to acetic acid, sialic acid, and trout water, but not

539   to proline and glycine (Baatrup & Døving, 1985). Several factors may contribute to these

540   differences. First, it is not entirely clear if Baatrup and Døving recorded from papillae or fimbriae

541   (see Cook et al., 1990 for details). If they recorded from fimbriae, their chemosensory response

542   profile may be different than the one from the papillae. We did not specifically investigate

543   fimbriae here, but we found that they contain SCCs with microvilli and that these cells are

544   innervated, contrary to earlier reports (Lethbridge & Potter, 1979). Second, oral and gill pore

545   papillae may have different chemosensory response profiles. Third, response profiles could be

546   species-specific as it is the case for the taste system that is tuned to the diet of the animal (Finger,

547   1997; Kasumyan & Døving, 2003). In both studies, trout water was a potent stimulus. The

23

548   stimulatory compounds of the trout water are not known yet. However, SCC responses to

549   individual chemicals from both our study and that of Baatrup & Døving (1985) suggest the

550   presence of amino acids, bile acids, and mucus-derived chemicals. These are likely to be found in

551   trout thawing water along with bacterial substances (see discussion below). This may indicate a

552   role in predator detection as teleosts can be predators of lampreys (Applegate, 1950; Potter,

553   1980; Vladykov, 1949) or it may indicate a role in feeding as sea lampreys feed on trout (Farmer,

554   1980; Lennon, 1954; Smith, 1971; Swink, 2003). Our findings support the latter hypothesis by

555   showing that amino acids (proline and glycine), which are generally considered as feeding-

556   associated cues in fish (Jones, 1989; Mackie & Mitchell, 1983; Mearns, 1986, 1989; Takeda, Takii,

557   & Matsui, 1984; Valentinčič & Caprio, 1994; for reviews see Finger, 1997; Kasumyan & Døving,

558   2003), induce excitatory responses in sea lamprey papillae. Moreover, these two amino acids are

559   concentrated in marine animal tissue (Beers, 1967; Carr, Netherton, Gleeson, & Derby, 1996) on

560   which sea lampreys feed. The responses to the bile acid taurocholic acid seen in the present study,

561   may corroborate a role of the SCC system in feeding as taurocholic acid is a potent stimulus of the

562   taste system in several fish species (Hara, 1994; Michel, 2005; Rolen & Caprio, 2008). However,

563   bile acids including taurocholic acid could act as social cues in fish (Li, Sorensen, & Gallahers, 1995;

564   Sorensen, Hara, & Stacey, 1991; Zhang & Hara, 2009). The failure of the lamprey pheromones

565   3kPZS or 3kACA to stimulate chemosensory responses in gill pore papillae could be due to the fact

566   that these sex pheromones are released at the gills (Siefkes, Scott, Zielinski, Yun, &, Li, 2003). This

567   would then result in a continuous stimulation of the receptors by the pheromones. The chemical

568   sensitivity of the lamprey SCC system is thus different from the olfactory system, which is highly

569   sensitive to basic amino acids (arginine and histidine) and pheromones (Green et al., 2017; Li,

570   1994) and at least partially different from that of the gustatory system that responds to

24

571   substances that are not stimulatory for the SCC system (sucrose, quinine) in *L. planeri* (Baatrup &

572   Døving, 1985).

573   Apart from lampreys, the chemical sensitivity of SCCs has been defined in only a few

574   species. In the sea robin (*Prionotus carolinus*), recordings of the spinal nerves innervating the free

575   pectoral fins rays that contain SCCs, showed responses to feeding-related cues such as prey

576   extract and amino acids (Silver & Finger, 1984). In rocklings (genus *Ciliata* and *Gaidropsarus*), the

577   SCCs of the anterior dorsal fin respond to body mucus of heterospecific fish, but not to classical

578   fish taste stimuli (amino-acids, etc.) or pheromones from congeners (Peters et al., 1987, 1991). In

579   the sea catfish (*Plotosus japonicus*), the maxillary barbels are extremely sensitive to pH variations

580   (Caprio, Shimohara, Marui, Harada, & Kiyohara, 2014) and to amino acids (Caprio et al., 2015).

581   However, the barbels contain both taste buds and SCCs which prevents the identification of the

582   sensory receptors involved (Caprio et al., 2014, 2015). In terrestrial vertebrates, SCCs have been

583   observed in amphibians, reptiles and mammals (Finger et al., 2003; Hansen, 2007; Sbarbati &

584   Osculati, 2003). However, their chemical sensitivity is only known in mammals where SCCs located

585   in the airways detect irritants and bacterial compounds via taste receptors (Finger et al., 2003;

586   Gulbransen, Clapp, Finger, & Kinnamon, 2008; Lin, Ogura, Margolskee, Finger, & Restrepo, 2008;

587   Tizzano et al., 2010). The detection of these substances by airways SCCs triggers different defense

588   mechanisms. The activation of SCC bitter and sweet taste receptors tunes the release of

589   antimicrobial peptide by adjacent epithelial cells (Lee et al., 2014, 2017). It also prevents harmful

590   airborne substances (irritants, toxins, etc.) to further enter the organism by evoking protective

591   respiratory reflexes (Finger et al., 2003) and by regulating fluid access to the vomeronasal organ

592   (Ogura, Krosnowski, Zhang, Bekkerman, & Lin, 2010). These findings suggest a third possible

593   interpretation of our results in lampreys. Indeed, the SCC-stimulating compound of the trout

25

594 water may be bacterial or irritants substances. Therefore the SCC system in lampreys could have

595 a similar role as in mammals.

596

597 **4.2 Innervation of cutaneous papillae and central projections**

598 Tracer injections in the different types of papillae demonstrated that the trigeminal nerve

599 innervates oral and nasal papillae, the glossopharyngeal and vagus nerves innervate gill pore

600 papillae, and spinal dorsal roots innervate dorsal fin papillae. Our tracing experiments did not

601 specifically label the sensory fibers innervating SCCs. Therefore, we cannot differentiate between

602 fibers innervating SCCs, Merkel cells, free nerve endings, or fibers innervating any other types of

603 receptors. However, all labeled fibers from one type of papillae entered the brainstem by the

604 same cranial nerve and had a similar projection pattern in the central nervous system. For

605 example, all labeled fibers from oral papillae which contain numerous SCCs and several Merkel

606 cells entered the brainstem through the trigeminal nerve and descended in the rdV to reach the

607 rostral spinal cord. However the size or diameter of the ganglion cells and axons differed. These

608 differences could relate to the different types of sensory fibers innervating the papillae, but more

609 information is needed to conclude on this matter. One exception to this pattern involves gill pore

610 papillae. On 2 animals out of 4, gill pore papillae injections labeled fibers that travelled in the

611 recurrent branch of the anterior lateral line nerve to enter the brainstem and terminate in the

612 dorsal nucleus of the octavolateral area, a nucleus mainly involved in electroreception (Bodznick

613 & Northcutt, 1981; Koyama, 2005; Ronan & Northcutt, 1987). Occasional putative skin

614 photoreceptors, referred to as "microvillous cells", have been reported on gill pore papillae

615 (Whitear & Lane, 1983b). Others have described similar cells on the tail of larvae and showed their

616 innervation by lateral line fibers (Steven, 1951; Whitear & Lane, 1983b). There is thus a small

617 possibility that the labeled lateral line fibers in our material could be innervating such cells.

618   However, the fibers innervating photoreceptor cells from the tail area of larval lampreys enter the

619   brainstem through the posterior lateral line nerve and terminate in the medial nucleus of the

620   octavolateral area (Ronan & Bodznick, 1991). Another possibility is that the lateral line fibers were

621   accidentally labeled by lesioning a neuromast, some of which are located in the vicinity of gill pore

622   papillae, slightly dorsal between the gill pores.

623   The source of SCC innervation is often inferred from their location on the body. However, only a

624   few studies identified the nerves providing innervation to SCCs. In sea robins, spinal nerves

625   provide innervation to the SCCs of the pectoral fin rays (Finger, 1997; Silver & Finger, 1984). In

626   rocklings, the dorsal recurrent branch of the facial nerve provides innervation to the SCCs of the

627   anterior dorsal fin, whereas spinal nerves provide innervation to other sensory cells (Merkel)

628   located on the same structure (Kotrschal & Whitear, 1988; Whitear & Kotrschal, 1988). In rodents,

629   the trigeminal nerve provides innervation to SCCs in the distal part of the airways (Finger et al.,

630   2003; Gulbransen, Silver, & Finger, 2008; Silver & Finger, 2009; Tizzano et al., 2010). Our results

631   in the lamprey support the view that cranial or spinal nerves providing cutaneous innervation to

632   the area where the SCCs are located also provide innervation to those SCCs (Fig. 9; Finger, 1997).

633   To our knowledge, the central projection pattern of the SCC system is only known from

634   the two teleosts species mentioned above, *Prionotus* and *Ciliata*. In *Prionotus*, the central

635   projections of the SCC system mirror those of an ascending somatosensory system, the dorsal

636   column system. The situation is different in rocklings where the SCCs are centrally connected like

637   an external taste system. Primary afferents terminate in the vagal lobe which, in turn, projects to

638   the secondary taste nucleus (Finger, 1997; Kotrschal & Finger, 1996). In lampreys, the central

639   projection pattern resembles that of the somatosensory system. The central process of the

640   trigeminal ganglion cells that innervate oral or nasal papillae courses in the descending root of

641   the trigeminal nerve (rdV). The central process of the glossopharyngeal or vagal ganglion cells that

27

642   innervate gill pore papillae courses caudally or rostrally in a longitudinal tract that is adjacent to

643   the rdV. Most of the fibers course caudally in that tract to reach the rostral spinal segments. A

644   few fibers course rostrally in the same tract to reach isthmic levels. We did not see any labeled

645   fibers in the rdV after gill pore papillae injections, suggesting that the fibers in the rdV in the whole

646   nIX/X labeling experiments do not innervate gill pore papillae. The central process of the dorsal

647   root ganglion cells that innervate dorsal fin papillae entered the dorsal columns through the

648   dorsal roots and then ran caudally and rostrally for a few segments. It is possible that the rostrally-

649   directed fibers reach brainstem levels directly, but it remains to be demonstrated.

650   We also specifically traced taste bud-innervating fibers from the periphery (i.e. taste buds)

651   to their central target. To our knowledge, this is the first time this has been done in lampreys since

652   previous studies were based on whole-nerve labeling (Fritzsch & Northcutt, 1993; Koyama, 2005).

653   The taste bud injections did not label fibers in the rdV as for whole nIX/X injections, suggesting

654   that the rdV fibers that course in nIX/X innervate structures other than taste buds and gill pore

655   papillae. We now show that the central projection of the lamprey taste system is different from

656   that of the SCC system. The fibers innervating the taste buds are of finer caliber and course in a

657   longitudinal tract located at the lateral edge of the alar plate. Along this tract, the fibers terminate

658   at all levels in a well-delineated nucleus, just medial to the tract, in the caudal hindbrain, but do

659   not reach spinal levels. Based on immunohistochemical data, previous studies have suggested

660   that this nucleus is the lamprey homologue of the mammalian nucleus of the solitary tract (NST)

661   (Auclair et al., 2004; Barreiro-Iglesias et al., 2010; Pombal et al., 2008, 2006; Robertson, Auclair,

662   Ménard, Grillner, & Dubuc, 2007). The present study strongly supports this hypothesis by showing

663   that this nucleus is the primary target of taste bud afferents in lampreys as in other vertebrates

664   (Beckstead, & Norgren, 1979; Contreras, Beckstead, & Norgren, 1982; Finger, 1987, 1997;

665   Hamilton & Norgren, 1984; Herrick, 1905; Norgren & Leonard, 1973). We also described that some

28

666   of the taste bud afferents ascend to terminate at isthmic levels. Other studies have reported such

667   ascending inputs from taste bud afferents in other species, but they only briefly discussed them

668   despite a potential role in central processing of taste inputs (rabbit: Hanamori & Smith, 1989; rat:

669   Hamilton & Norgren, 1984; frog: Hanamori & Ishiko, 1983; Matesz & Székely, 1978; chicken:

670   Ganchrow, Gentle, & Ganchrow, 1987).

671

672   **4.3 Evolutionary considerations and conclusion**

673   Taken together, our results show that lampreys, the most basal extant group of

674   vertebrates, possess a relatively well developed and distributed SCC system that is particularly

675   well represented on cutaneous papillae. Lamprey SCCs were found in all locations where they

676   have been reported in other species. Our results confirm that the cranial or spinal nerves

677   responsible for the cutaneous innervation of an area also provide innervation to SCCs in the same

678   area. The gill pore papillae respond mainly to trout-derived chemicals and amino acids, which

679   could indicate a role in feeding, in predator avoidance or in protective behaviors. The lamprey SCC

680   system appears less specialized than the highly specialized SCC systems observed in *Prionotus* and

681   *Ciliata* and may resemble the ancestral SCC system from which more specialized systems may

682   have arisen. The SCC system is also associated to a variety of behaviors in vertebrates: feeding,

683   predator avoidance, or detection of bacteria and irritants. Altogether, these differences between

684   taxa in the morphology, distribution, chemical sensitivity, and associated behavioral function raise

685   the question of the homology of SCCs among vertebrates. For instance, nasal SCCs in mammals

686   are often considered as components of an array of taste-like cells that are distributed throughout

687   the gut and airways (Saunders et al., 2014). These cells share molecular similarity and use a similar

688   transduction pathway (Saunders, Reynolds, & Finger, 2013). However, SCCs in fish do not seem

689   to use a G protein-coupled receptor transduction cascade as taste bud cells (Ohmoto, Okada,

29

690   Nakamura, Abe, & Matsumoto, 2011). Furthermore, important differences can exist among

691   species of the same vertebrate lineage. For example, in fish, SCCs located on the trunk are

692   innervated either by spinal or cranial nerves (*Prionotus*, Finger, 1997; Silver & Finger, 1984;

693   *Gaidropsarus*, *Ciliata*, Kotrschal & Whitear, 1988; Whitear & Kotrschal, 1988). So far, these

694   differences have been mainly attributed to phylogenetic differences. They may also be due to the

695   anatomical location of the SCCs. Indeed, in each species examined so far, the SCCs were located

696   on a different body location: anterior dorsal fin in *Ciliata*; fin rays in *Prionotus*, and airways in

697   mammals. The lamprey model offers the opportunity to test the hypothesis that SCC function may

698   be linked to their location. It will also provide a unique framework to shed light on SCC homology

699   in vertebrates and to compare the respective territories of the taste and SCC systems.

700

701

Author Contributions

703   GD, BZ, and RD designed the study; GD, FB, FA, TS, JL-B, and MM performed the experiments; GD,

704   FB, FA, analyzed the data; GD, FA, BZ and RD wrote the paper.

705

706

References

708   Albersheim-Carter, J., Blubaum, A., Ballagh, I. H., Missaghi, K., Siuda, E. R., McMurray, G., Bass, A.

709   H., Dubuc, R., Kelley, D. B., Schmidt, M. F., Wilson, R. J., & Gray, P.A. (2016). Testing the

710   evolutionary conservation of vocal motoneurons in vertebrates. *Respiratory physiology &*

711   *neurobiology, 224*, 2-10. doi:10.1016/j.resp.2015.06.010.

30

712   Applegate, V. C. (1950). Natural history of the sea lamprey (*Petromyzon marinus*) in Michigan.

713   *Spec   Sci   Rep   US   Fish   Wildl   Serv,   55,   1-237.   Retrieved   from*

714   http://name.umdl.umich.edu/2142335.0001.001

715   Auclair, F., Lund, J. P., & Dubuc, R. (2004). Immunohistochemical distribution of tachykinins in the

716   CNS of the lamprey *Petromyzon marinus*. *Journal of Comparative Neurology*, *479*(3), 328-346. doi:

717   10.1002/cne.20324

718   Baatrup, E., & Døving, K. B. (1985). Physiological studies on solitary receptors of the oral disc

719   papillae in the adult brook lamprey, *Lampetra planeri* (Bloch). *Chemical senses*, *10*(4), 559-566.

720   doi:10.1093/chemse/10.4.559

721   Bardach, J. E., & Case, J. (1965). Sensory capabilities of the modified fins of squirrel hake

722   (*Urophycis chuss*) and searobins (*Prionotus carolinus* and *P. evolans*). *Copeia, 2*, 194-206.

723   doi:10.2307/1440724

724   Barreiro-Iglesias, A., Anadón, R., & Rodicio, M. C. (2010). The gustatory system of lampreys. *Brain,*

725   *behavior and evolution, 75*(4), 241-250. doi:10.1159/000315151

726   Beamish, R. J. (2010). The use of gill pore papillae in the taxonomy of lampreys. *Copeia, 2010*(4),

727   618-628. doi:10.1643/CI-09-107

728   Beckstead, R. M., & Norgren, R. (1979). An autoradiographic examination of the central

729   distribution of the trigeminal, facial, glossopharyngeal, and vagal nerves in the monkey. *Journal*

730   *of Comparative Neurology, 184*(3), 455-472. doi: 10.1002/cne.901840303

731   Beers, J. R. (1967). The species distribution of some naturally-occurring quaternary ammonium

732   compounds. *Comparative   Biochemistry   and   Physiology,   21*(1),   11-21.   doi:10.1016/0010-

733   406X(67)90109-0

31

734   Bodznick, D., & Northcutt, R. G. (1981). Electroreception in lampreys: evidence that the earliest

735   vertebrates were electroreceptive. *Science, 212*(4493), 465-467. doi:10.1126/science.7209544

736   Braun, C. B. (1996). The sensory biology of the living jawless fishes: a phylogenetic assessment.

737   *Brain, Behavior and Evolution, 48*(5), 262-276. doi:10.1159/000113205

738   Braun, C. B. (1998). Schreiner organs: a new craniate chemosensory modality in hagfishes. *Journal

739   of Comparative Neurology, 392*(2), 135-163. doi:10.1002/(SICI)1096-

740   9861(19980309)392:2<135::AID-CNE1>3.0.CO;2-3

741   Braun, C. B., & Northcutt, R. G. (1998). Cutaneous exteroreceptors and their innervation in

742   hagfishes. In J. M. Jørgensen, J. P. Lomholt, R. E. Weber, & H. Malte (Eds.), *The biology of hagfishes*

743   (pp. 512-532). Dordrecht: Springer.

744   Caprio, J., Shimohara, M., Marui, T., Harada, S., & Kiyohara, S. (2014). Marine teleost locates live

745   prey through pH sensing. *Science, 344*(6188), 1154-1156. doi: 10.1126/science.1252697

746   Caprio, J., Shimohara, M., Marui, T., Kohbara, J., Harada, S., & Kiyohara, S. (2015). Amino acid

747   specificity of fibers of the facial/trigeminal complex innervating the maxillary barbel in the

748   Japanese sea catfish, *Plotosus japonicus*. *Physiology & Behavior, 152*, 288-294. doi:

749   10.1016/j.physbeh.2015.10.011

750   Carr, W. E., Netherton, III, J. C., Gleeson, R. A., & Derby, C. D. (1996). Stimulants of feeding

751   behavior in fish: analyses of tissues of diverse marine organisms. *The Biological Bulletin, 190*(2),

752   149-160. doi:10.2307/1542535

753   Codina, E., Loïc, K., Compere, P., Dragičević, B., Dulčić, J., & Parmentier, E. (2012). The barbel-like

754   specialization of the pelvic fins in *Ophidion rochei* (Ophidiidae). *Journal of Morphology, 273*(12),

755   1367-1376. doi:10.1002/jmor.20066

32

756 Contreras, R. J., Beckstead, R. M., & Norgren, R. (1982). The central projections of the trigeminal,

757 facial, glossopharyngeal and vagus nerves: an autoradiographic study in the rat. *Journal of the*

758 *Autonomic Nervous System, 6*(3), 303-322. doi:10.1016/0165-1838(82)90003-0

759 Cook, R. D., Hilliard, R. W., & Potter, I. C. (1990). Oral papillae of adults of the southern hemisphere

760 lamprey *Geotria australis. Journal of Morphology, 203*(1), 87-96. doi:10.1002/jmor.1052030109

761 Daghfous, G., Green, W. W., Zielinski, B. S., & Dubuc, R. (2012). Chemosensory-induced motor

762 behaviors in fish. *Current Opinion in Neurobiology, 22*(2), 223-230.

763 doi:10.1016/j.conb.2011.10.009

764 Dawson, J. (1905). The breathing and feeding mechanism of the lampreys. *The Biological Bulletin,*

765 *9*(1), 1-21. doi:10.2307/1535799

766 Fahrenholz, C. (1936a). Tastzellen und Tastorgane in der Neunaugenhaut. *Zeitschrift fur*

767 *mikroskopisch-anatomische Forschung*, *39*, 116-134.

768 Fahrenholz, C. (1936b). Die sensiblen Einrichtungen der Neunaugenhaut. *Zeitschrift fur*

769 *mikroskopisch-anatomische Forschung*, *40*, 323-380.

770 Farmer, G. J. (1980). Biology and physiology of feeding in adult lampreys. *Canadian Journal of*

771 *Fisheries and Aquatic Sciences, 37*(11), 1751-1761. doi:10.1139/f80-220

772 Ficalbi, E. (1914). Struttura del tegumento dei Petromizonti. *Archivio italiano di Anatomia e di*

773 *Embriologia, 12*, 596-827.

774 Finger, T. E. (1982). Somatotopy in the representation of the pectoral fin and free fin rays in the

775 spinal cord of the sea robin, *Prionotus carolinus*. *The Biological Bulletin*, *163*(1), 154-161.

776 doi:10.2307/1541505

777   Finger, T.E. (1987). Gustatory nuclei and pathways in the central nervous system. In T. E. Finger,

778   & W. L. Silver (Eds.), *Neurobiology of Taste and Smell* (pp. 285-310). New York: John Wiley & Sons.

779   Finger, T. E. (1997). Evolution of taste and solitary chemoreceptor cell systems. *Brain, Behavior*

780   *and Evolution*, *50*(4), 234-243. doi:10.1159/000113337

781   Finger, T. E. (2000). Ascending spinal systems in the fish, *Prionotus carolinus*. *Journal of*

782   *Comparative   Neurology,   422*(1),   106-122.   doi:10.1002/(SICI)1096-

783   9861(20000619)422:1<106::AID-CNE7>3.0.CO;2-T

784   Finger, T. E., Böttger, B., Hansen, A., Anderson, K. T., Alimohammadi, H., & Silver, W. L. (2003).

785   Solitary chemoreceptor cells in the nasal cavity serve as sentinels of respiration. *Proceedings of*

786   *the National Academy of Sciences, 100*(15), 8981-8986. doi:10.1073/pnas.1531172100

787   Foettinger, A. (1876). Recherches sur la structure de l'épiderme des Cyclostomes et quelques

788   mots sur les cellules olfactives de ces animaux. *Bulletin de l'Académie Royale de Belgique. Série 2.*

789   Fox, H., Lane, E. B., & Whitear, M. (1980). Sensory nerve endings and receptors in fish and

790   amphibians. In R. I. C. Spearman, & P. A. Riley (Eds), *The Skin of Vertebrates*, Linnean Society

791   Symposium Series 9 (pp. 271–281). London: Academic Press.

792   Fritzsch, B., & Northcutt, G. (1993). Cranial and spinal nerve organization in amphioxus and

793   lampreys: evidence for an ancestral craniate pattern. *Cells Tissues Organs, 148*(2-3), 96-109.

794   doi:10.1159/000147529

795   Fusari, R. (1907). Contributo allo studio dei nervi cutanei e delle terminazioni nervöse nella cute

796   e nella mucose orale dell'"*Ammocoetes branchialis*". *Atti della Accademia delle Scienze di Torino,*

797   *42*, 192-200.

798   Ganchrow, D., Gentle, M. J., & Ganchrow, J. R. (1987). Central distribution and efferent origins of

799   facial nerve branches in the chicken. *Brain Research Bulletin, 19*(2), 231-238. doi:10.1016/0361-

800   9230(87)90088-8

801   Greeley, J. R. (1927). Fishes of the Oswego watershed. In State of New York Conservation

802   Department*, A biological survey of the Oswego River system*. Supplemental to Seventeenth annual

803   report (pp. 84-107). Albany: JB Lyon Company.

804   Green, W. W., Boyes, K., McFadden, C., Daghfous, G., Auclair, F., Zhang, H., & Zielinski, B. S. (2017).

805   Odorant organization in the olfactory bulb of the sea lamprey. *Journal of Experimental Biology,*

806   *220*(7), 1350-1359. doi:10.1242/jeb.150466

807   Gulbransen, B. D., Clapp, T. R., Finger, T. E., & Kinnamon, S. C. (2008). Nasal solitary

808   chemoreceptor cell responses to bitter and trigeminal stimulants in vitro. *Journal of*

809   *Neurophysiology, 99*(6), 2929-2937. doi:10.1152/jn.00066.2008

810   Gulbransen, B., Silver, W., & Finger, T. E. (2008). Solitary chemoreceptor cell survival is

811   independent of intact trigeminal innervation. *Journal of Comparative Neurology, 508*(1), 62-71.

812   doi:10.1002/cne.21657

813   Hamilton, R. B., & Norgren, R. (1984). Central projections of gustatory nerves in the rat. *Journal*

814   *of Comparative Neurology, 222*(4), 560-577. doi: 10.1002/cne.902220408

815   Hanamori, T., & Ishiko, N. (1983). Intraganglionic distribution of the primary afferent neurons in

816   the frog glossopharyngeal nerve and its transganglionic projection to the rhombencephalon

817   studied by HPR method. *Brain Research, 260*(2), 191-199. doi:10.1016/0006-8993(83)90674-1

818   Hanamori, T., & Smith, D. V. (1989). Gustatory innervation in the rabbit: central distribution of

819   sensory and motor components of the chorda tympani, glossopharyngeal, and superior laryngeal

820   nerves. *Journal of Comparative Neurology, 282*(1), 1-14. doi:10.1002/cne.902820102

821   Hansen, A. (2007). Olfactory and solitary chemosensory cells: two different chemosensory

822   systems in the nasal cavity of the American alligator, *Alligator mississippiensis*. *BMC Neuroscience,*

823   *8,* 64. doi:10.1186/1471-2202-8-64

824   Hansen, A., Ghosal, R., Caprio, J., Claus, A., & Sorensen, P. (2014). Anatomical and physiological

825   studies of bigheaded carps demonstrate that the epibranchial organ functions as a pharyngeal

826   taste organ. *Journal of Experimental Biology, 217,* 3945-3954. doi:10.1242/jeb.107870

827   Hansen, A., & Reutter, K. (2004). Chemosensory systems in fish: structural, functional and

828   ecological aspects. In G. von der Emde, J. Mogdans, & B. G. Kapoor (Eds.), *The senses of fish* (pp.

829   55-89). Dordrecht: Springer.

830   Hara, T. J. (1994). Olfaction and gustation in fish: an overview. *Acta Physiologica Scandinavica*,

831   *152*(2), 207-217. doi:10.1111/j.1748-1716.1994.tb09800.x

832   Herrick, C. J. (1905). The central gustatory paths in the brains of bony fishes. *Journal of*

833   *Comparative Neurology and Psychology, 15*(5), 375-456. doi:10.1002/cne.920150503

834   Jones, K. A. (1989). The palatability of amino acids and related compounds to rainbow trout, *Salmo*

835   *gairdneri* Richardson. *Journal of Fish Biology, 34*(1), 149-160. doi:10.1111/j.1095-

836   8649.1989.tb02964.x

837   Kasumyan, A. O., & Døving, K. B. (2003). Taste preferences in fishes. *Fish and Fisheries, 4*(4), 289-

838   347. doi:10.1046/j.1467-2979.2003.00121.x

839   Khidir, K. T., & Renaud, C. B. (2003). Oral fimbriae and papillae in parasitic lampreys

840   (Petromyzontiformes). *Environmental Biology of Fishes, 66*(3), 271-278.

841   doi:10.1023/A:1023961910547

842   Kirino, M., Parnes, J., Hansen, A., Kiyohara, S., & Finger, T. E. (2013). Evolutionary origins of taste

843   buds: phylogenetic analysis of purinergic neurotransmission in epithelial chemosensors. *Open*

844   *Biology, 3*(3), 130015. doi:10.1098/rsob.130015

845   Kölliker, A. (1885). Stiftchenzellen in der Epidermis von Froschlarven. *Zoologischer Anzeiger, 8*,

846   439-441.

847   Kölliker, A. (1886). Histologische Studien an Batrachierlarven. *Zeitschrift für wissenschaftliche*

848   *Zoologie, 43*, 1-40.

849   Kotrschal, K. (1991). Solitary chemosensory cells—taste, common chemical sense or what?

850   *Reviews in Fish Biology and Fisheries, 1*(1), 3-22. doi:10.1007/BF00042659

851   Kotrschal, K. (1992). Quantitative scanning electron microscopy of solitary chemoreceptor cells in

852   cyprinids and other teleosts. *Environmental Biology of Fishes, 35*(3), 273-282.

853   doi:10.1007/BF00001894

854   Kotrschal, K. (1995). Ecomorphology of solitary chemosensory cell systems in fish: a review.

855   *Environmental Biology of Fishes, 44*, 143-155. doi:10.1007/BF00005912

856   Kotrschal, K. (1996). Solitary chemosensory cells: why do primary aquatic vertebrates need

857   another taste system? *Trends in Ecology & Evolution, 11*(3), 110-114. doi:10.1016/0169-

858   5347(96)81088-3

859   Kotrschal, K., & Finger, T. E. (1996). Secondary connections of the dorsal and ventral facial lobes

860   in a teleost fish, the rockling (*Ciliata mustela*). *Journal of Comparative Neurology, 370*(4), 415-426.

861   doi:10.1002/(SICI)1096-9861(19960708)370:4<415::AID-CNE1>3.0.CO;2-7

862   Kotrschal, K., Krautgartner, W. D., & Hansen, A. (1997). Ontogeny of the solitary chemosensory

863   cells in the zebrafish, *Danio rerio*. *Chemical senses, 22*(2), 111-118. doi:10.1093/chemse/22.2.111

864   Kotrschal, K., Peters, R., & Atema, J. (1989). A novel chemosensory system in fish: do rocklings

865   (*Ciliata mustela*, Gadidae) use their solitary chemoreceptor cells as fish detectors. *The Biological*

866   *Bulletin, 177*, 328. Retrieved from http://www.jstor.org/stable/1541946

867   Kotrschal, K., Peters, R., & Atema, J. (1993). Sampling and behavioral evidence for mucus

868   detection in a unique chemosensory organ: the anterior dorsal fin in rocklings (*Ciliata mustela*:

869   Gadidae: Teleostei). *Zoologische Jahrbücher. Abteilung für allgemeine Zoologie und Physiologie*

870   *der Tiere, 97*(1), 47-67.

871   Kotrschal, K., Royer, S., & Kinnamon, J. C. (1998). High-voltage electron microscopy and 3-D

872   reconstruction of solitary chemosensory cells in the anterior dorsal fin of the Gadid fish *Ciliata*

873   *mustela* (Teleostei). *Journal of structural biology, 124*(1), 59-69. doi:10.1006/jsbi.1998.4046

874   Kotrschal, K., & Whitear, M. (1988). Chemosensory anterior dorsal fin in rocklings (*Gaidropsarus*

875   and *Ciliata*, teleostei, Gadidae): Somatotopic representation of the ramus recurrens facialis a

876   revealed by transganglionic transport of HRP. *Journal of Comparative Neurology, 268*(1), 109-120.

877   doi:10.1002/cne.902680111

878   Kotrschal, K., Whitear, M., & Adam, H. (1984). Morphology and histology of the anterior dorsal fin

879   of *Gaidropsarus mediterra*neus (Pisces Teleostei), a specialized sensory organ. *Zoomorphology,*

880   *104*(6), 365-372. doi:10.1007/BF00312187

38

881   Kotrschal, K., Whitear, M., & Finger, T. E. (1993). Spinal and facial innervation of the skin in the

882   gadid fish *Ciliata mustela* (Teleostei). *Journal of Comparative Neurology, 331*(3), 407-417.

883   doi:10.1002/cne.903310310

884   Koyama, H. (2005). Organization of the sensory and motor nuclei of the glossopharyngeal and

885   vagal nerves in lampreys. *Zoological Science, 22*(4), 469-476. doi:10.2108/zsj.22.469

886   Koyama, H., Kishida, R., Goris, R. C., & Kusunoki, T. (1990). Organization of the primary projections

887   of the lateral line nerves in the lamprey *Lampetra japonica*. *Journal of Comparative Neurology,*

888   *295*(2), 277-289. doi:10.1002/cne.902950210

889   Koyama, H., Nagai, T., Takeuchi, H. A., & Hillyard, S. D. (2001). The spinal nerves innervate putative

890   chemosensory cells in the ventral skin of desert toads, *Bufo alvarius*. *Cell and Tissue Research,*

891   *304*(2), 185-192. doi:10.1007/s004410100370

892   Kuciel, M., Lauriano, E. R., Silvestri, G., Żuwała, K., Pergolizzi, S., & Zaccone, D. (2014). The

893   structural organization and immunohistochemistry of G-protein alpha subunits in the olfactory

894   system of the air-breathing mudskipper, *Periophthalmus barbarus* (Linnaeus, 1766) (Gobiidae,

895   Oxudercinae). *Acta Histochemica, 116*(1), 70-78. doi:10.1016/j.acthis.2013.05.005

896   Lane, E. B., & Whitear, M. (1982). Sensory structures at the surface of fish skin: I. Putative

897   chemoreceptors. *Zoological Journal of the Linnean Society, 75*(2), 141-151. doi:10.1111/j.1096-

898   3642.1982.tb01944.x

899   Langerhans, P. (1873). *Untersuchungen über Petromyzon planeri*. Universitätsbuchhandlung von

900   Carl Trommer.

901   Lee, R. J., Hariri, B. M., McMahon, D. B., Chen, B., Doghramji, L., Adappa, N. D., Palmer, J. N.,

902   Kennedy, D. W., Jiang, P., Margolskee, R. F., & Cohen, N. A. (2017). Bacterial d-amino acids

39

903   suppress sinonasal innate immunity through sweet taste receptors in solitary chemosensory cells.

904   *Science Signaling*, *10*(495), eaam7703. doi:10.1126/scisignal.aam7703.

905   Lee, R. J., Kofonow, J. M., Rosen, P. L., Siebert, A. P., Chen, B., Doghramji, L., Xiong, G., Adappa, N.

906   D., Palmer, J. N., Kennedy, D. W., Kreindler, J. L., Margolskee, R. F., & Cohen, N. A. (2014). Bitter

907   and sweet taste receptors regulate human upper respiratory innate immunity. *The Journal of*

908   *Clinical Investigation, 124*(3), 1393-1405. doi:10.1172/JCI72094

909   Lennon, R. E. (1954). Feeding mechanism of the sea lamprey and its effect on host fishes. *Fishery*

910   *Bulletin   of   the   US   Fish   and   Wildlife   Service,   56*(98),   247-293.   Retrieved   from

911   http://spo.nmfs.noaa.gov/content/feeding-mechanism-sea-lamprey-and-its-effect-host-fishes

912   Lethbridge, R. C., & Potter, I. C. (1979). The oral fimbriae of the lamprey *Geotria australis*. *Journal*

913   *of Zoology, 188*(2), 267-277. doi:10.1111/j.1469-7998.1979.tb03404.x

914   Lethbridge, R.C., & Potter, I.C. (1981). The skin. In M. W. Hardisty, & I. C. Potter (Eds.), *The biology*

915   *of lampreys.* Vol. 3 (pp. 377-448). London: Academic Press.

916   Li, W. (1994). *The olfactory biology of adult sea lamprey (Petromyzon marinus)* (Doctoral

917   dissertation, University of Minnesota). Available from ProQuest Dissertations and Theses

918   database. (UMI No. 9514669)

919   Li, W., Sorensen, P. W., & Gallaher, D. D. (1995). The olfactory system of migratory adult sea

920   lamprey (*Petromyzon marinus*) is specifically and acutely sensitive to unique bile acids released

921   by   conspecific   larvae.   *The   Journal   of   general   physiology*,   *105*(5),   569-587.

922   doi:10.1085/jgp.105.5.569

923   Lin, W., Ogura, T., Margolskee, R. F., Finger, T. E., & Restrepo, D. (2008). TRPM5-expressing solitary

924   chemosensory cells respond to odorous irritants. *Journal of Neurophysiology, 99*(3), 1451-1460.

925   doi:10.1152/jn.01195.2007

926   Linnaeus, C. V. (1758). *Systema Naturae per regna tria naturae, secundum classes, ordines,*

927   *genera, species, cum characteribus, differentiis, synonymis, locis*. (10th ed.). Holmiae [Stockholm]:

928   Impensis Direct.

929   Mackie, A. M., & Mitchell, A. I. (1983). Studies on the chemical nature of feeding stimulants for

930   the juvenile European eel, *Anguilla anguilla* (L.). *Journal of Fish Biology, 22*(4), 425-430.

931   doi:10.1111/j.1095-8649.1983.tb04764.x

932   Marenghi, G. (1903). Alcune particolarita di struttura e di innervazione della cute

933   dell'*Ammocoetes branchialis*. *Memoria letta nella seduta del 9. Iuglio 1903.* U. Hoepli.

934   Matesz, C., & Székely, G. (1978). The motor column and sensory projections of the branchial

935   cranial nerves in the frog. *Journal of Comparative Neurology, 178*(1), 157-175.

936   doi:10.1002/cne.901780109

937   Mearns, K. J. (1986). Sensitivity of brown trout (*Salmo trutta* L.) and Atlantic salmon (*Salmo salar*

938   L.) fry to amino acids at the start of exogenous feeding. *Aquaculture, 55*(3), 191-200.

939   doi:10.1016/0044-8486(86)90114-6

940   Mearns, K. J. (1989). Behavioural responses of salmonid fry to low amino acid concentrations.

941   *Journal of Fish Biology, 34*(2), 223-232. doi:10.1111/j.1095-8649.1989.tb03304.x

942   Michel, W. C. (2005). Chemoreception. In D. H. Evans & J. B. Claiborne (Eds.), *The Physiology of*

943   *Fishes* (3rd Ed; pp. 471-498). Boca Raton: CRC Press.

944   Morrill, A. D. (1895). The pectoral appendages of *Prionotus* and their innervation. *Journal of*

945   *Morphology, 11*(1), 177-192. doi:10.1002/jmor.1050110105

946   Nagai, T., Koyama, H., Von Seckendorff Hoff, K., & Hillyard, S. D. (1999). Desert toads discriminate

947   salt taste with chemosensory function of the ventral skin. *Journal of Comparative Neurology,*

948   *408*(1), 125-136. doi:10.1002/(SICI)1096-9861(19990524)408:1<125::AID-CNE9>3.0.CO;2-0

949   Norgren, R., & Leonard, C. M. (1973). Ascending central gustatory pathways. *Journal of*

950   *Comparative Neurology, 150*(2), 217-237. doi:10.1002/cne.901500208

951   Ogura, T., Krosnowski, K., Zhang, L., Bekkerman, M., & Lin, W. (2010). Chemoreception regulates

952   chemical access to mouse vomeronasal organ: role of solitary chemosensory cells. *PLoS One, 5*(7),

953   e11924. doi:10.1371/journal.pone.0011924

954   Ohmoto, M., Okada, S., Nakamura, S., Abe, K., & Matsumoto, I. (2011). Mutually exclusive

955   expression of Gαia and Gα14 reveals diversification of taste receptor cells in zebrafish. *Journal of*

956   *Comparative Neurology*, *519*(8), 1616-1629. doi: 10.1002/cne.22589

957   Osculati, F., & Sbarbati, A. (1995). The frog taste disc: a prototype of the vertebrate gustatory

958   organ. *Progress in Neurobiology, 46*(4), 351-399. doi:10.1016/0301-0082(95)00006-H

959   Parker, G. H. (1912). The relation of smell, taste, and the common chemical sense in vertebrates.

960   *Proceedings of the Academy of Natural Sciences of Philadelphia, 15*, 221-234. Retrieved from

961   https://catalog.hathitrust.org/Record/012241821

962   Peach, M. B. (2005). New microvillous cells with possible sensory function on the skin of sharks.

963   *Marine   and   Freshwater   Behaviour   and   Physiology,   38*(4),   275-279.

964   doi:10.1080/10236240500482416

42

965   Peters, R. C., Kotrschal, K., & Krautgartner, W. D. (1991). Solitary chemoreceptor cells of *Ciliata*

966   *mustela* (Gadidae, Teleostei) are tuned to mucoid stimuli. *Chemical Senses, 16*(1), 31-42.

967   doi:10.1093/chemse/16.1.31

968   Peters, R. C., Van Steenderen, G. W., & Kotrschal, K. (1987). A chemoreceptive function for the

969   anterior dorsal fin in rocklings (*Gaidropsarus* and *Ciliata*: Teleostei: Gadidae): electrophysiological

970   evidence. *Journal of the Marine Biological Association of the United Kingdom, 67*(4), 819-823.

971   doi:10.1017/S0025315400057064

972   Pombal, M. A., López, J. M., de Arriba, M. C., González, A., & Megías, M. (2008). Distribution of

973   adrenomedullin-like immunoreactivity in the brain of the adult sea lamprey. *Brain Research*

974   *Bulletin, 75*(2-4), 261-265. doi: 10.1016/j.brainresbull.2007.10.011

975   Pombal, M. A., López, J. M., de Arriba, M. C., Megías, M., & González, A. (2006). Distribution of

976   neuropeptide FF-like immunoreactive structures in the lamprey central nervous system and its

977   relation to catecholaminergic neuronal structures. *Peptides*, *27*(5), 1054-1072.

978   doi:10.1016/j.peptides.2005.06.033

979   Potter, I. C. (1980). Ecology of larval and metamorphosing lampreys. *Canadian Journal of Fisheries*

980   *and Aquatic Sciences, 37*(11), 1641-1657. doi:10.1139/f80-212

981   Potter, I. C., Lanzing, W. J. R., & Strahan, R. (1968). Morphometric and meristic studies on

982   populations of Australian lampreys of the genus *Mordacia*. *Journal of the Linnean Society of*

983   *London, Zoology, 47*(313), 533-546. doi:10.1111/j.1096-3642.1968.tb00550f.x

984   Pouzat, C., Mazor, O., & Laurent, G. (2002). Using noise signature to optimize spike-sorting and to

985   assess neuronal classification quality. *Journal of Neuroscience Methods, 122*(1), 43-57.

986   doi:10.1016/S0165-0270(02)00276-5

43

987   Retzius, G. (1892). Die Nervenendigungen in dem Geschmacksorgan der Säugethiere und

988   Amphibien. In *Biologische Untersuchungen: Neue Folge* Vol. IV (pp. 26-32). Stockholm: Samson &

989   Wallin.

990   Robertson, B., Auclair, F., Ménard, A., Grillner, S., & Dubuc, R. (2007). GABA distribution in lamprey

991   is   phylogenetically   conserved.   *Journal   of   Comparative   Neurology,   503*(1),   47-63.

992   doi:10.1002/cne.21348

993   Rodríguez-Alonso, R., Megías, M., Pombal, M. A., & Molist, P. (2017). Morphological and

994   functional aspects of the epidermis of the sea lamprey *Petromyzon marinus* throughout

995   development. *Journal of Fish Biology, 91*(1), 80-100. doi:10.1111/jfb.13330

996   Rolen, S. H., & Caprio, J. (2008). Bile salts are effective taste stimuli in channel catfish. *Journal of

997   Experimental Biology*, *211*(17), 2786-2791. doi:10.1242/jeb.018648

998   Ronan, M., & Bodznick, D. (1991). Behavioral and neurophysiological demonstration of a lateralis

999   skin photosensitivity in larval sea lampreys. *Journal of Experimental Biology, 161*(1), 97-117.

1000   Retrieved from http://jeb.biologists.org/content/161/1/97

1001   Ronan, M., & Northcutt, R. G. (1987). Primary projections of the lateral line nerves in adult

1002   lampreys. *Brain, Behavior and Evolution, 30*(1-2), 62-81. doi:10.1159/000118638

1003   Rovainen, C. M., & Yan, Q. (1985). Sensory responses of dorsal cells in the lamprey brain. *Journal

1004   of Comparative Physiology A, 156*(2), 181-183. doi:10.1007/BF00610859

1005   Saunders, C. J., Christensen, M., Finger, T. E., & Tizzano, M. (2014). Cholinergic neurotransmission

1006   links solitary chemosensory cells to nasal inflammation. *Proceedings of the National Academy of

1007   Sciences, 111*(16), 6075-6080. doi:10.1073/pnas.1402251111

44

1008   Saunders, C. J., Reynolds, S. D., & Finger, T. E. (2013). Chemosensory brush cells of the trachea. A

1009   stable population in a dynamic epithelium. *American Journal of Respiratory Cell and Molecular*

1010   *Biology, 49*(2), 190-196. doi: 10.1165/rcmb.2012-0485OC

1011   Sbarbati, A., Crescimanno, C., Benati, D., & Osculati, F. (1998). Solitary chemosensory cells in the

1012   developing chemoreceptorial epithelium of the vallate papilla. *Journal of Neurocytology, 27*(9),

1013   631-635. doi:10.1023/A:1006933528084

1014   Sbarbati, A., Crescimanno, C., Bernardi, P., & Osculati, F. (1999). α-gustducin-immunoreactive

1015   solitary chemosensory cells in the developing chemoreceptorial epithelium of the rat vallate

1016   papilla. *Chemical Senses, 24*(5), 469-472. doi:10.1093/chemse/24.5.469

1017   Sbarbati, A., & Osculati, F. (2003). Solitary chemosensory cells in mammals? *Cells Tissues Organs,*

1018   *175*(1), 51-55. doi:10.1159/000073437

1019   Siefkes, M. J., Scott, A. P., Zielinski, B., Yun, S. S., & Li, W. (2003). Male sea lampreys, *Petromyzon*

1020   *marinus* L., excrete a sex pheromone from gill epithelia. *Biology of Reproduction, 69*(1), 125-132.

1021   doi:10.1095/biolreprod.102.014472

1022   Silver, W. L., & Finger, T. E. (1984). Electrophysiological examination of a non-olfactory, non-

1023   gustatory chemosense in the searobin, *Prionotus carolinus*. *Journal of Comparative Physiology A:*

1024   *Neuroethology, Sensory, Neural, and Behavioral Physiology, 154*(2), 167-174.

1025   doi:10.1007/BF00604982

1026   Silver, W. L., & Finger, T. E. (2009). The anatomical and electrophysiological basis of peripheral

1027   nasal trigeminal chemoreception. *Annals of the New York Academy of Sciences, 1170*(1), 202-205.

1028   doi:10.1111/j.1749-6632.2009.03894.x

1029   Smith, B. R. (1971). Sea lampreys in the Great Lakes of North America. In M. W. Hardisty, & I. C.

1030   Potter (Eds.), *The biology of lampreys*. Vol. 1 (pp. 207-247). London: Academic Press Inc.

1031   Sorensen, P. W., Hara, T. J., & Stacey, N. E. (1991). Sex pheromones selectively stimulate the

1032   medial olfactory tracts of male goldfish. *Brain Research*, *558*(2), 343-347. doi:10.1016/0006-

1033   8993(91)90790-3

1034   Steven, D. M. (1951). Sensory cells and pigment distribution in the tail of the ammocoete. *Journal*

1035   *of Cell Science, 3*(19), 233-247. Retrieved from http://jcs.biologists.org/content/s3-92/19/233

1036   Studnička, F. K. (1913). Epidermoidale Sinneszellen bei jungen Ammocoeten (Proammocoeten).

1037   *Anatomischer   Anzeiger,   44*(5),   102-112.   Retrieved   from

1038   http://archive.org/details/anatomischeranze44anat/page/102

1039   Suntres, T. E., Daghfous, G., Dubuc, R. D., & Zielinski, B. S. (this issue). Gill solitary chemosensory

1040   cells during the complex life cycle of the sea lamprey, *Petromyzon marinus*. *Journal of*

1041   *Comparative Neurology*.

1042   Swink, W. D. (2003). Host selection and lethality of attacks by sea lampreys (*Petromyzon marinus*)

1043   in laboratory studies. *Journal of Great Lakes Research, 29*, 307-319. doi:10.1016/S0380-

1044   1330(03)70496-1

1045   Takahashi-Iwanaga, H., & Abe, K. (2001). Scanning electron microscopic observation of Merkel

1046   cells in the lamprey epidermis. *Kaibogaku Zasshi, 76*(4), 375-380.

1047   Takeda, M., Takii, K., & Matsui, K. (1984). Identification of feeding stimulants for juvenile eel.

1048   *Nippon Suisan Gakkaishi, 50*(4), 645-651. doi:10.2331/suisan.50.645

1049   Tizzano, M., & Finger, T. E. (2013). Chemosensors in the nose: guardians of the airways.

1050   *Physiology, 28*(1), 51-60. doi:10.1152/physiol.00035.2012

46

1051   Tizzano, M., Gulbransen, B. D., Vandenbeuch, A., Clapp, T. R., Herman, J. P., Sibhatu, H. M., &

1052   Finger, T. E. (2010). Nasal chemosensory cells use bitter taste signaling to detect irritants and

1053   bacterial signals. *Proceedings of the National Academy of Sciences, 107*(7), 3210-3215.

1054   doi:10.1073/pnas.0911934107

1055   Tizzano, M., Merigo, F., & Sbarbati, A. (2006). Evidence of solitary chemosensory cells in a large

1056   mammal: the diffuse chemosensory system in *Bos taurus* airways. *Journal of Anatomy, 209*(3),

1057   333-337. doi:10.1111/j.1469-7580.2006.00617.x

1058   Tretjakoff, D. (1927). Das Nervensystem des Flussnevnauges. *Zeitschrift für wissenschaftliche*

1059   *Zoologie, 129*, 359-452.

1060   Turton, W. (1803). *A general system of nature, through the three grand kingdoms of animals,*

1061   *vegetables, and minerals; with their habitations, manners, economy, structure, and pecularities*.

1062   (Translated from Linnaeus, C. V. (1788) Systema naturæ (12th ed)). London: Lackington, Allen &

1063   Co.

1064   Valentinčič, T., & Caprio, J. (1994). Consummatory feeding behavior to amino acids in intact and

1065   anosmic channel catfish *Ictalurus punctatus*. *Physiology & Behavior, 55*(5), 857-863.

1066   doi:10.1016/0031-9384(94)90071-X

1067   Vladykov, V. D. (1949). *Quebec Lampreys (Petromyzonidae): I. List of Species and Their Economical*

1068   *Importance* (Vol. 26, pp. 1-67). Québec: Department of Fisheries.

1069   Whitear, M. (1952). The innervation of the skin of teleost fishes. *Journal of Cell Science, 3*(23),

1070   289-306. Retrieved from http://jcs.biologists.org/content/s3-93/23/289

1071   Whitear, M. (1965). Presumed sensory cells in fish epidermis. *Nature, 208*(5011), 703-704.

1072   doi:10.1038/208703b0

1073   Whitear, M. (1971). Cell specialization and sensory function in fish epidermis. *Journal of Zoology*,

1074   *163*(2), 237-264. doi:10.1111/j.1469-7998.1971.tb04533.x

1075   Whitear, M. (1976). Identification of the epidermal "Stiftchenzellen" of frog tadpoles by electron

1076   microscopy. *Cell and Tissue Research, 175*(3), 391-402. doi:10.1007/BF00218717

1077   Whitear, M. (1989). Merkel cells in lower vertebrates. *Archives of Histology and Cytology,*

1078   *52*(Supplement), 415-422. doi:10.1679/aohc.52.Suppl_415

1079   Whitear, M. (1992). Solitary chemosensory cells. In T. J. Hara (Ed), *Fish Chemoreception* (pp. 103-

1080   125). Dordrecht: Springer.

1081   Whitear, M., & Kotrschal, K. (1988). The chemosensory anterior dorsal fin in rocklings

1082   (*Gaidropsarus* and *Ciliata*, Teleostei, Gadidae): activity, fine structure and innervation. *Journal of*

1083   *Zoology, 216*(2), 339-366. doi:10.1111/j.1469-7998.1988.tb02434.x

1084   Whitear, M., & Lane, E. B. (1981). Fine structure of Merkel cells in lampreys. *Cell and Tissue*

1085   *Research, 220*(1), 139-151. doi:10.1007/BF00209973

1086   Whitear, M., & Lane, E. B. (1983a). Oligovillous cells of the epidermis: sensory elements of lamprey

1087   skin. *Journal of Zoology, 199*(3), 359-384. doi:10.1111/j.1469-7998.1983.tb02102.x

1088   Whitear, M., & Lane, E. B. (1983b). Multivillous cells: epidermal sensory cells of unknown function

1089   in lamprey skin. *Journal of Zoology, 201*(2), 259-272. doi:10.1111/j.1469-7998.1983.tb04275.x

1090   Whitear, M., & Moate, R. M. (1994). Chemosensory cells in the oral epithelium of *Raja clavata*

1091   (Chondrichthyes). *Journal of Zoology, 232*(2), 295-312. doi:10.1111/j.1469-7998.1994.tb01574.x

1092   Woodland, W. N. F. (1913). On the supposed gnathostome ancestry of the Marsipobranchii; with

1093   a brief description of some features of the gross anatomy of the genera *Geotria* and *Mordacia*.

48

1094   *Anatomischer   Anzeiger,   45*(5),   113-153.   Retrieved   from

1095   https://www.biodiversitylibrary.org/item/43340

1096   Zhang, C., & Hara, T. J. (2009). Lake char (*Salvelinus namaycush*) olfactory neurons are highly

1097   sensitive and specific to bile acids. *Journal of Comparative Physiology A*, *195*(2), 203-215.

1098   doi:10.1007/s00359-008-0399-y

1099

1100

1101   Figure Legends

1102   **Figure 1.** Location of cutaneous papillae in spawning adult sea lampreys. (a) Schematic illustration

1103   of *Petromyzon marinus* showing the anatomical location of the cutaneous papillae (adapted from

1104   Greeley, 1927). Papillae are present around the oral disc, on the skin bordering the nostril, on the

1105   posterior margin of the gill pores, and on the dorsal fins (arrows). (b) to (e) are stereomicrographs

1106   of cutaneous papillae illustrated at a high magnification. (b) Arrowheads point to oral papillae on

1107   the external border of the oral disc. The flat skin extensions with digit-like protrusions at their tip

1108   located immediately behind the papillae are termed fimbriae and were not investigated in the

1109   present study. (c) Nasal papillae are arranged around the lip of the nostril. (d) Papillae form a

1110   dorso-ventral row along the posterior margin of a gill pore. (e) Papillae extend from the surface

1111   of the anterior dorsal fin, forming a fringe its trailing edge. Scale bars = 1000 μm (b), 250 μm (c),

1112   400 μm (d), and 200 μm (e).

1113

1114   **Figure 2.** SEMs of the surface of oral, nasal, gill pore, and dorsal fin papillae. (a1) Low power image

1115   of an oral papilla showing the distribution of microvillar tufts over its surface. (a2) Higher power

1116   image of a portion of an oral papilla showing examples of microvillar tufts over its surface. (a3)

49

1117   High power image of one microvillar tuft on an oral papilla. (b1) Low power image of three

1118   adjacent nasal papillae showing the distribution of microvillar tufts over their surface. (b2) Higher

1119   power image of a portion of a nasal papilla showing examples of microvillar tufts over its surface.

1120   (b3) High power image of one microvillar tuft on a nasal papilla. (c1) Low power image of two

1121   adjacent gill pore papillae showing the distribution of microvillar tufts over their surface. (c2)

1122   Higher power image of a portion of a gill pore papilla showing examples of microvillar tufts over

1123   its surface. (c3) High power image of one microvillar tuft on a gill pore papilla. (d1) Low power

1124   image of two adjacent dorsal fin papillae showing the distribution of microvillar tufts over their

1125   surface. (d2) Higher power image of a portion of a dorsal fin papilla showing examples of

1126   microvillar tufts over its surface. (d3) High power image of one microvillar tuft on a dorsal fin

1127   papilla. Scale bars: (a1-d1) = 25 μm; (a2-d2) = 5 μm; (a3-d3) = 2 μm.

1128

1129   **Figure 3.** Epifluorescence photomicrographs of whole mounts and sectioned oral, nasal, gill pore,

1130   and dorsal fin papillae showing the binding of phalloidin. Examination under high power was used

1131   to identify SCCs (arrows) and Merkel cells (arrowheads). (a1) Photomicrograph of an oral papilla

1132   (whole mount) showing the numerous tufts of microvilli over its surface. The microvilli were

1133   revealed by the binding of green fluorescent phalloidin. (a2-a4) Photomicrographs of oral papillae

1134   cut along their long axis showing examples of SCCs with microvilli (arrows) and Merkel cells

1135   (arrowheads). Only a few SCCs (magenta arrow in (a2)) were sectioned in such a way that allowed

1136   for the observation of their whole typical elongated piriform shape. The microvilli were revealed

1137   by the binding of green fluorescent phalloidin. (b1) Photomicrograph of a nasal papilla (whole

1138   mount) showing a few tufts of microvilli over its surface. The microvilli were revealed by the

1139   binding of green fluorescent phalloidin. (b2-b4) Photomicrographs of sections of nasal papillae

1140   along their long axis showing a few examples of SCCs with microvilli (arrows) and many examples

1141   of Merkel cells (arrowheads). The inset in (b2) shows numerous Merkel cells (arrowheads) at the

1142   tip of a nasal papilla. The microvilli were revealed by the binding of green fluorescent phalloidin.

1143   (c1) Photomicrograph of a gill pore papilla (whole mount) showing the numerous tufts of microvilli

1144   over its surface. The microvilli were revealed by the binding of green fluorescent phalloidin. (c2-

1145   c4) Photomicrographs of sections of gill pore papillae along their long axis (c2 and c4) and on a

1146   cross section (c3) showing examples of SCCs with microvilli (arrows) and one Merkel cell

1147   (arrowhead in (c4)). Only a few SCCs (magenta arrows in (c3 and c4)) were sectioned in such a

1148   way that allowed for the observation of their whole typical elongated piriform shape. The

1149   microvilli were revealed by the binding of green fluorescent phalloidin. (d1) Photomicrograph of

1150   a dorsal fin papilla (whole mount) showing a few tufts of microvilli over its surface. The microvilli

1151   were revealed by the binding of green fluorescent phalloidin. (d2-d4) Photomicrographs of

1152   sections of dorsal fin papillae along their long axis showing examples of SCCs with microvilli

1153   (arrows) and Merkel cells (arrowheads). Only a few SCCs (magenta arrows in (d3 and d4)) were

1154   sectioned in such a way that allowed for the observation of their whole typical elongated piriform

1155   shape. The microvilli were revealed by the binding of green fluorescent phalloidin. The scale bar

1156   in (d1) is for (a1,b1,c1,d1) and the one in (d4) is for (a2-a4, b2-b4, c2-c4, d2-d4); both = 50 μm.

1157

1158   **Figure 4.** Neural responses of gill pore papillae to chemical stimulation. **Top:** Schematic illustration

1159   of the experimental recording procedure showing the location of the gill pore papillae, the

1160   recording electrode and the chemical stimulus delivery system. Scale bar = 25 μm. **Bottom:**

1161   Examples of multiunit activity recorded from gill pore papillae in response to delivery of different

1162   chemical stimuli. (+) indicates a significantly increased activity; (-) indicates a significantly

1163   decreased activity; (0) indicates no significant change in activity. Arrowheads indicate chemical

1164   delivery onset. The chemical stimuli tested included trout water, amino acids, sialic acid (a mucus

51

1165   component), taurocholic acid (a bile acid), 3-keto allocholic acid (3kACA) and 3-keto petromyzonol

1166   sulfate (3kPZS) (sex pheromones), and Ringer's solution (control solution). The responses are

1167   illustrated as rasters of three consecutive responses with the associated peristimulus time

1168   histogram (PSTH). See **Table 3** for response statistics and a detailed trial by trial analysis.

1169

1170   **Figure 5.** Central projections of trigeminal afferents that innervate oral and nasal papillae. The top

1171   panel shows a schematic illustration of a dorsal view of the hindbrain showing the extent of the

1172   central projections from oral and nasal papillae (blue line). Transverse gray lines represent the

1173   levels of the cross sections illustrated in the photomicrographs in the bottom section of the figure.

1174   A green fluorescent Nissl stain was used as counterstain. (a1) Fluorescence photomicrograph of a

1175   cross section corresponding to level (a1) from the top panel. Fibers labeled from an injection of

1176   biocytin in oral papillae (white arrows) enter the brainstem through the trigeminal sensory root

1177   (nVs) and then join the descending root of the trigeminal nerve (rdV). (b1) The fibers from the

1178   same animal described in (a1) are shown here (between the white arrows) descending in the rdV

1179   on a cross section corresponding to level (b1) from the top panel. (c1) The fibers described in (a1)

1180   and (b1) are shown here (between the white arrows) descending in the rdV on a cross section

1181   corresponding to level (c1) from the top panel. (a2) Fluorescence photomicrograph of a cross

1182   section corresponding to level (a2) from the top panel. Fibers labeled from an injection of biocytin

1183   in nasal papillae (white arrows) enter the brainstem through the trigeminal sensory root (nVs) and

1184   join the descending root of the trigeminal nerve (rdV). Asterisks indicate autofluorescent blood

1185   vessels. (b2) The fibers from the same animal described in (a2) are shown here (between the

1186   white arrows) descending in the rdV on a cross section corresponding to level (b2) from the top

1187   panel. Asterisks indicate autofluorescent blood vessels. (c2) The fibers described in (a2) and (b2)

1188   are shown here (between the white arrows) descending in the rdV on a cross section

52

1189   corresponding to level (c2) from the top panel. Asterisks indicate autofluorescent blood vessels.

1190   Inset photomicrographs in (c1) and (c2) illustrate trigeminal ganglion cells labeled in the

1191   maxillomandibular nerve ganglion ($gV_{2,3}$) after oral papillae injections (c1) and in the ophthalmicus

1192   profundus nerve ganglion (gV_1) after nasal papillae injections (c2). ARRN, anterior

1193   rhombencephalic reticular nucleus; d, dorsal; DC, dorsal column nucleus; l, lateral; Mes,

1194   mesencephalon; nIX, glossopharyngeal nerve; nllp, posterior lateral line nerve; NOMA, anterior

1195   octavomotor nucleus; NOMP, posterior octavomotor nucleus; nVm, motor root of the trigeminal

1196   nerve; nVs, sensory root of the trigeminal nerve; rdV, descending root of the trigeminal nerve; Rh,

1197   rhombencephalon; SC, spinal cord; V, trigeminal motor nucleus; X, vagal motor nucleus. Scale bars

1198   over photomicrographs = 200 µm.

1199

1200   **Figure 6.** Photomicrographs of cross sections of papillae and pharyngeal taste buds showing their

1201   innervation. Note that the magenta labeling at the surface of the tissue in (a), (b) and (d) is

1202   unspecific autofluorescence. The green channel in (a), (b) and (e) is fluorescent Nissl staining while

1203   in (c) and (d), it is phalloidin labeling. (a,b,c) Injecting the trigeminal nerve at its exit from the

1204   cranium labeled fibers (arrowheads) innervating the oral (a) and nasal (c) papillae, and the oral

1205   fimbriae (b). In (c), many Merkel cells are indicated with white arrows and one out-of-focus SCC

1206   is indicated with a magenta arrow. (d) Injecting the glossopharyngeal or vagus nerves at their exit

1207   from the cranium labeled fibers (arrowheads) innervating the gill pore papillae. Labeled microvilli

1208   from two SCCs are indicated with magenta arrows. (e) Injecting the glossopharyngeal and vagus

1209   nerves at their exit from the cranium also labeled fibers (arrowheads) innervating pharyngeal

1210   taste buds. Scale bars = 50 µm.

1211

53

1212   **Figure 7.** Central projections of glossopharyngeal and vagal afferents that innervate gill pore

1213   papillae or pharyngeal taste buds. The top panel shows a schematic illustration of a dorsal view

1214   of the hindbrain and the extent of the central projections from gill pore papillae (green) and taste

1215   buds (magenta). Transverse gray lines represent the levels of the cross sections illustrated in the

1216   photomicrographs in the bottom section of the figure. (a1,b1,c1) Photomicrographs of cross

1217   sections showing the central distribution of afferents (magenta, indicated with white arrows)

1218   labeled after gill pore papillae injection at three different rostro-caudal levels (see top panel for

1219   reference). The counterstain is a fluorescent Nissl stain (green). The fibers entered the brainstem

1220   through the glossopharyngeal (b1) and vagus nerves. Some fibers ascended to reach isthmic levels

1221   (a1) while other fibers descended in the caudal hindbrain (c1) on their way to the spinal cord. The

1222   inset in (b1) shows some glossopharyngeal ganglion cells labeled after gill pore papillae injection.

1223   (a2,b2,c2) Central distribution of afferents labeled after injection of a few pharyngeal taste buds

1224   (magenta, indicated with white arrows) for comparison with gill pore papillae afferents shown in

1225   (a1,b1,c1). The counterstain used here is fluorescent Nissl stain (green). Rostro-caudal levels of

1226   the cross sections illustrated in photomicrographs in panels (a2,b2,c2) correspond to the levels of

1227   panels (a1,b1,c1), respectively. The labeled taste bud afferents entered the brainstem through

1228   the glossopharyngeal nerve (b2) and vagus nerve, and many terminated in the nucleus of the

1229   solitary tract (NTS, b2), adjacent to the lateral edge of the alar plate. Some fibers ascended to

1230   reach isthmic levels (a2), while other fibers descended along the lateral edge of the alar plate (c2)

1231   to reach the caudal hindbrain. The inset in (c2) shows examples of glossopharyngeal ganglion cells

1232   labeled after taste bud injection. (a3,b3,c3) Whole nerve labeling showing the central distribution

1233   of all afferents from the vagus and glossopharyngeal nerves for comparison with gill pore papillae

1234   (a1,b1,c1) and taste bud (a2,b2,c2) afferents. Rostro-caudal levels of the cross sections illustrated

1235   in photomicrographs in panels (a3,b3,c3) correspond to the levels of panels (a1,b1,c1) and

54

1236   (a2,b2,c2), respectively (see also top panel for reference). The arrowheads in (b3) indicate axons

1237   from motoneurons on their way to exit the brainstem. The white arrows in (c3) indicate a central

1238   rootlet of the vagus nerve on its way to join the other taste bud afferents more dorsally located.

1239   The counterstain is DAPI, which labels nuclear DNA in blue. For all photomicrographs in the figure,

1240   we have delineated each afferent component with a specific color (see color code in the top panel

1241   for reference). Note that the whole nerve reference injection of glossopharyngeal and vagus

1242   nerves (a3,b3,c3) also labeled sensory fibers entering by the posterior lateral line nerve and the

1243   first spinal nerve, as indicated. ARRN, anterior rhombencephalic reticular nucleus; d, dorsal; DC,

1244   dorsal column nucleus; gIX, glossopharyngeal nerve ganglion; l, lateral; Mes, mesencephalon; nIX,

1245   glossopharyngeal nerve; nllp, posterior lateral line nerve; NOMA, anterior octavomotor nucleus;

1246   NOMP, posterior octavomotor nucleus; NTS, nucleus of the solitary tract; nVm, motor root of the

1247   trigeminal nerve; nVs, sensory root of the trigeminal nerve; nX, vagus nerve; rdV, descending root

1248   of the trigeminal nerve; Rh, rhombencephalon; SC, spinal cord; V, trigeminal motor nucleus; X,

1249   vagal motor nucleus. Scale bars for photomicrographs = 200 μm.

1250

1251   **Figure 8.** Central projections of dorsal root ganglion cells that innervate dorsal fin papillae. The

1252   top panel shows a schematic illustration of a dorsal view of the spinal cord showing the extent of

1253   the central projections from dorsal fin papillae (purple lines). Transverse gray lines represent the

1254   levels of the cross sections illustrated in the photomicrographs in the bottom section of the figure.

1255   (a,b,c,d) Photomicrographs of cross sections of the spinal cord and surrounding area at levels

1256   corresponding to levels (a) to (d) on the diagram, showing the labeling resulting from dorsal fin

1257   papillae injections. (a) Photomicrograph of a cross section of the spinal cord and surrounding area

1258   showing two ganglion cells (arrows) located dorsal to the spinal cord, and labeled fibers

1259   (arrowhead) in the dorsal columns of the spinal cord. Asterisks were placed over unlabeled

1260   ganglion cells. (b) Same as (a) but the labeled ganglion cell (arrow) is located ventral to the spinal

1261   cord. Labeled fibers are seen in the dorsal columns (arrowheads) and an asterisk was placed over

1262   an unlabeled ganglion cell. (c,d) Same as (a) but the ganglion cells (arrows) are located within the

1263   spinal canal. Labeled fibers are found in the dorsal columns (arrowheads). No counterstain was

1264   applied. dr, dorsal root; SC, spinal cord; vr, ventral root. Scale bar for all photomicrographs = 200

1265   µm.

1266

1267   **Figure 9**. The cutaneous papillae innervation and central projections. Top: Schematic illustration

1268   of a dorsal view of the hindbrain (left) and caudal spinal cord (right) showing the extent of the

1269   central projections from nasal (blue), oral (blue), gill pore (magenta), and fin (purple) papillae.

1270   Bottom: Schematic illustration of a lateral view of the head (left) and tail (right) of an adult

1271   spawning sea lamprey showing the location of the cutaneous papillae as well as their innervation

1272   by cranial and spinal nerves. The nasal and oral papillae are innervated by trigeminal afferents;

1273   the gill pore papillae are innervated by glossopharyngeal and vagus afferents; the fin papillae are
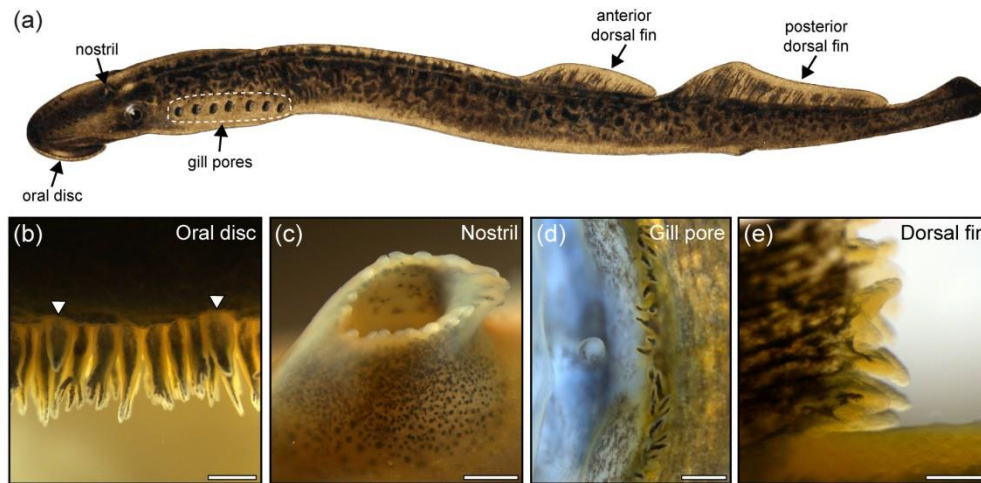
1274   innervated by spinal dorsal roots afferents.

56

Figure 1. Location of cutaneous papillae in spawning adult sea lampreys. (a) Schematic illustration of Petromyzon marinus showing the anatomical location of the cutaneous papillae (adapted from Greeley, 1927). Papillae are present around the oral disc, on the skin bordering the nostril, on the posterior margin of the gill pores, and on the dorsal fins (arrows). (b) to (e) are stereomicrographs of cutaneous papillae illustrated at a high magnification. (b) Arrowheads point to oral papillae on the external border of the oral disc. The flat skin extensions with digit-like protrusions at their tip located immediately behind the papillae are termed fimbriae and were not investigated in the present study. (c) Nasal papillae are arranged around the lip of the nostril. (d) Papillae form a dorso-ventral row along the posterior margin of a gill pore. (e) Papillae extend from the surface of the anterior dorsal fin, forming a fringe its trailing edge. Scale bars = 1000 μm (b), 250 μm (c), 400 μm (d), and 200 μm (e).

173x84mm (300 x 300 DPI)
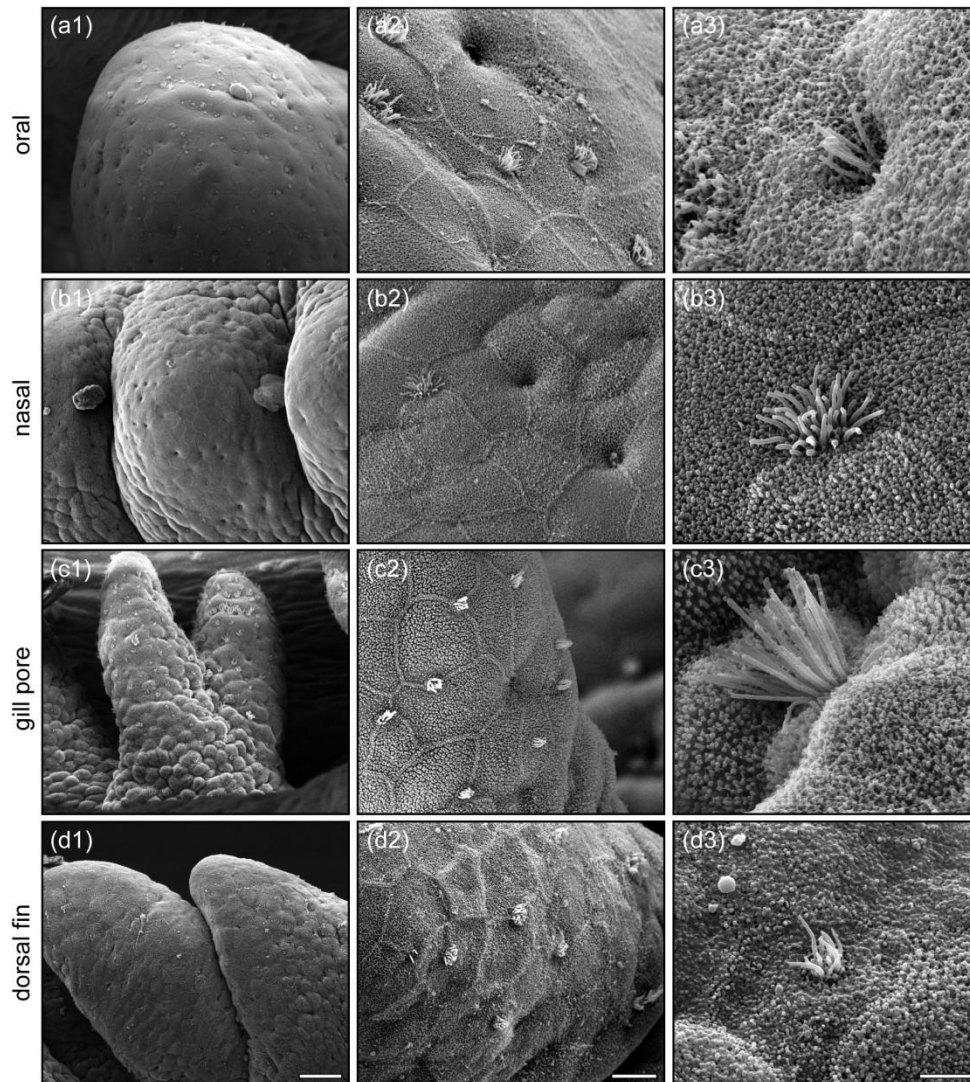
Figure 2. SEMs of the surface of oral, nasal, gill pore, and dorsal fin papillae. (a1) Low power image of an oral papilla showing the distribution of microvillar tufts over its surface. (a2) Higher power image of a portion of an oral papilla showing examples of microvillar tufts over its surface. (a3) High power image of one microvillar tuft on an oral papilla. (b1) Low power image of three adjacent nasal papillae showing the distribution of microvillar tufts over their surface. (b2) Higher power image of a portion of a nasal papilla showing examples of microvillar tufts over its surface. (b3) High power image of one microvillar tuft on a nasal papilla. (c1) Low power image of two adjacent gill pore papillae showing the distribution of microvillar tufts over their surface. (c2) Higher power image of a portion of a gill pore papilla showing examples of microvillar tufts over its surface. (c3) High power image of one microvillar tuft on a gill pore papilla. (d1) Low power image of two adjacent dorsal fin papillae showing the distribution of microvillar tufts over their surface. (d2) Higher power image of a portion of a dorsal fin papilla showing examples of microvillar tufts over its surface. (d3) High power image of one microvillar tuft on a dorsal fin papilla. Scale bars: (a1-d1) = 25 μm; (a2-d2) = 5 μm; (a3-d3) = 2 μm.
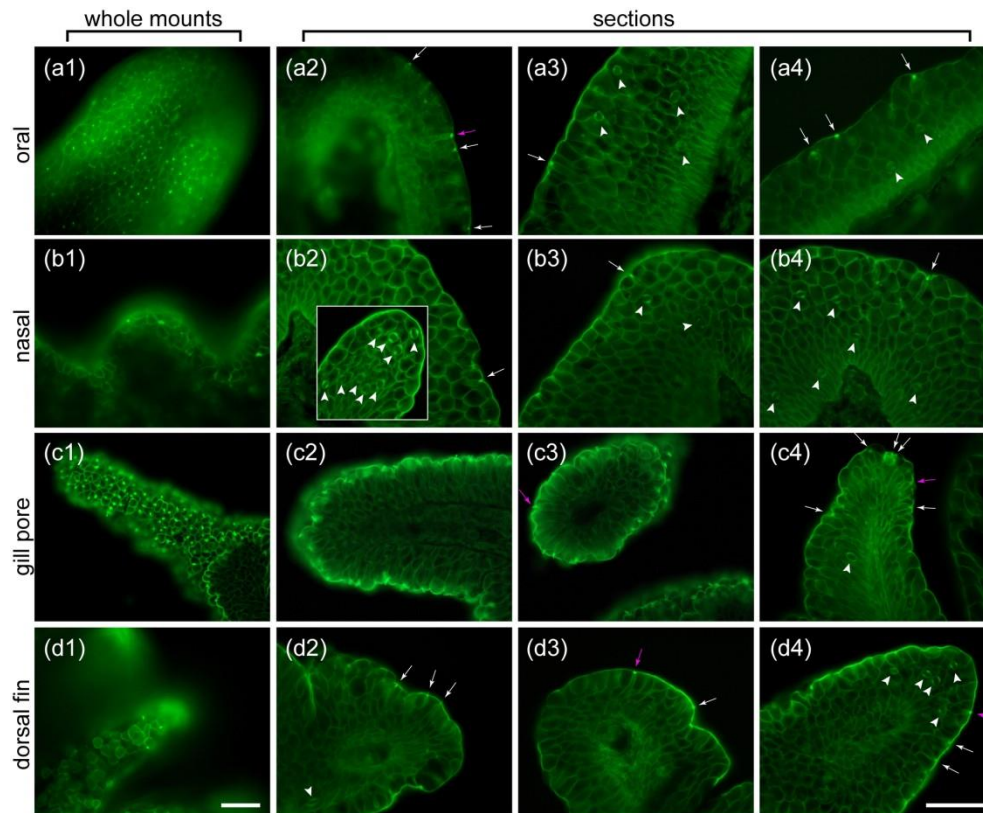
176x195mm (300 x 300 DPI)

Figure 3. Epifluorescence photomicrographs of whole mounts and sectioned oral, nasal, gill pore, and dorsal fin papillae showing the binding of phalloidin. Examination under high power was used to identify SCCs (arrows) and Merkel cells (arrowheads). (a1) Photomicrograph of an oral papilla (whole mount) showing the numerous tufts of microvilli over its surface. The microvilli were revealed by the binding of green fluorescent phalloidin. (a2-a4) Photomicrographs of oral papillae cut along their long axis showing examples of SCCs with microvilli (arrows) and Merkel cells (arrowheads). Only a few SCCs (magenta arrow in (a2)) were sectioned in such a way that allowed for the observation of their whole typical elongated piriform shape. The microvilli were revealed by the binding of green fluorescent phalloidin. (b1) Photomicrograph of a nasal papilla (whole mount) showing a few tufts of microvilli over its surface. The microvilli were revealed by the binding of green fluorescent phalloidin. (b2-b4) Photomicrographs of sections of nasal papillae along their long axis showing a few examples of SCCs with microvilli (arrows) and many examples of Merkel cells (arrowheads). The inset in (b2) shows numerous Merkel cells (arrowheads) at the tip of a nasal papilla. The microvilli were revealed by the binding of green fluorescent phalloidin. (c1) Photomicrograph of a gill pore papilla (whole mount) showing the numerous tufts of microvilli over its surface. The microvilli were revealed by the binding of green fluorescent phalloidin. (c2-c4) Photomicrographs of sections of gill pore papillae along their long axis (c2 and c4) and on a cross section (c3) showing examples of SCCs with microvilli (arrows) and one Merkel cell (arrowhead in (c4)). Only a few SCCs (magenta arrows in (c3 and c4)) were sectioned in such a way that allowed for the observation of their whole typical elongated piriform shape. The microvilli were revealed by the binding of green fluorescent phalloidin. (d1) Photomicrograph of a dorsal fin papilla (whole mount) showing a few tufts of microvilli over its surface. The microvilli were revealed by the binding of green fluorescent phalloidin. (d2-d4) Photomicrographs of sections of dorsal fin papillae along their long axis showing examples of SCCs with microvilli (arrows) and Merkel cells (arrowheads). Only a few SCCs (magenta arrows in (d3 and d4)) were sectioned in such a way that allowed for the observation of their typical elongated piriform shape. The microvilli were revealed by the binding of green fluorescent phalloidin. The scale bar in (d1) is for (a1,b1,c1,d1) and the one in (d4) is for (a2-a4, b2-b4, c2-c4, d2-d4); both = 50 µm.
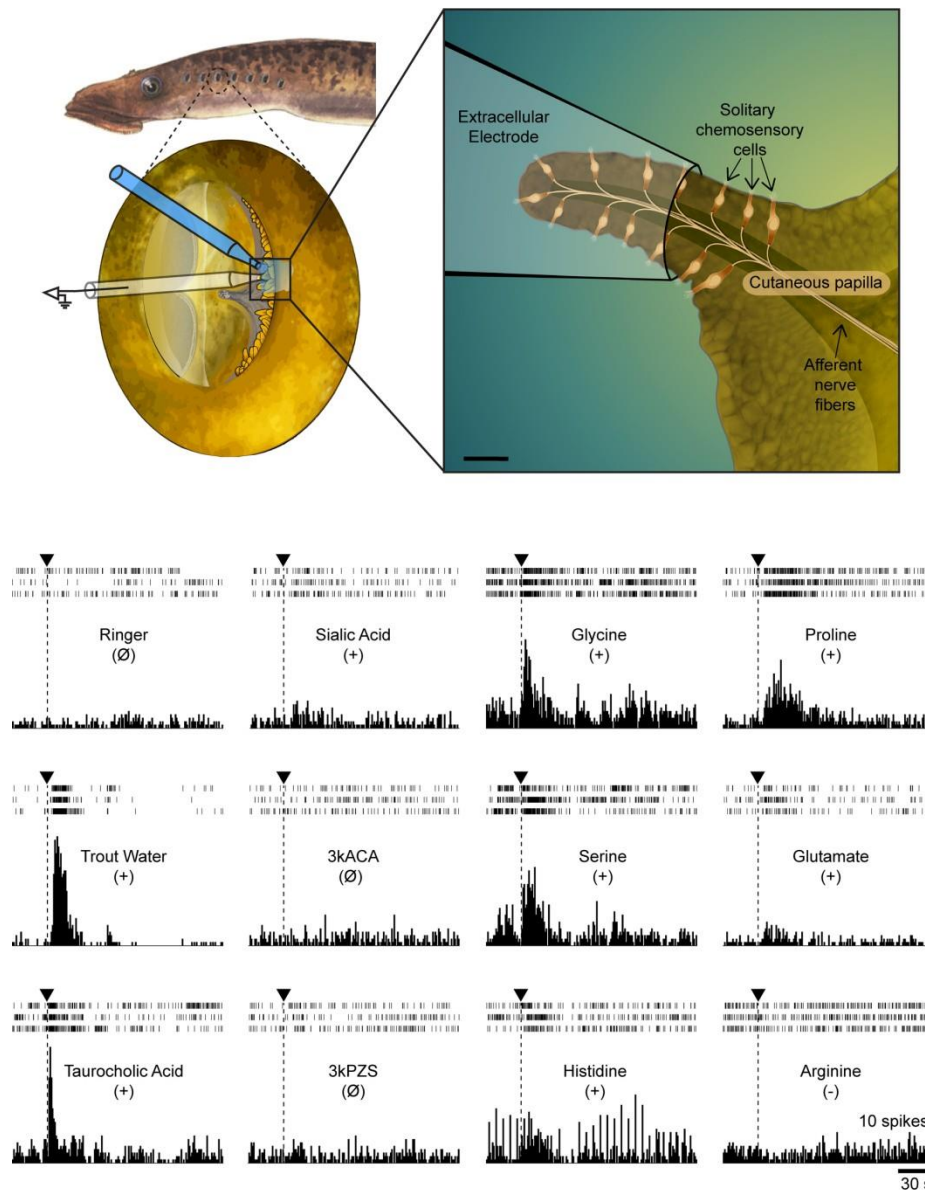
180x148mm (300 x 300 DPI)

Figure 4. Neural responses of gill pore papillae to chemical stimulation. Top: Schematic illustration of the experimental recording procedure showing the location of the gill pore papillae, the recording electrode and the chemical stimulus delivery system. Scale bar = 25 μm. Bottom: Examples of multiunit activity recorded from gill pore papillae in response to delivery of different chemical stimuli. (+) indicates a significantly increased activity; (-) indicates a significantly decreased activity; (0) indicates no significant change in activity. Arrowheads indicate chemical delivery onset. The chemical stimuli tested included trout water, amino acids, sialic acid (a mucus component), taurocholic acid (a bile acid), 3-keto allocholic acid (3kACA) and 3-keto petromyzonol sulfate (3kPZS) (sex pheromones), and Ringer's solution (control solution). The responses are illustrated as rasters of three consecutive responses with the associated peristimulus time histogram (PSTH). See **Table 3** for response statistics and a detailed trial by trial analysis.
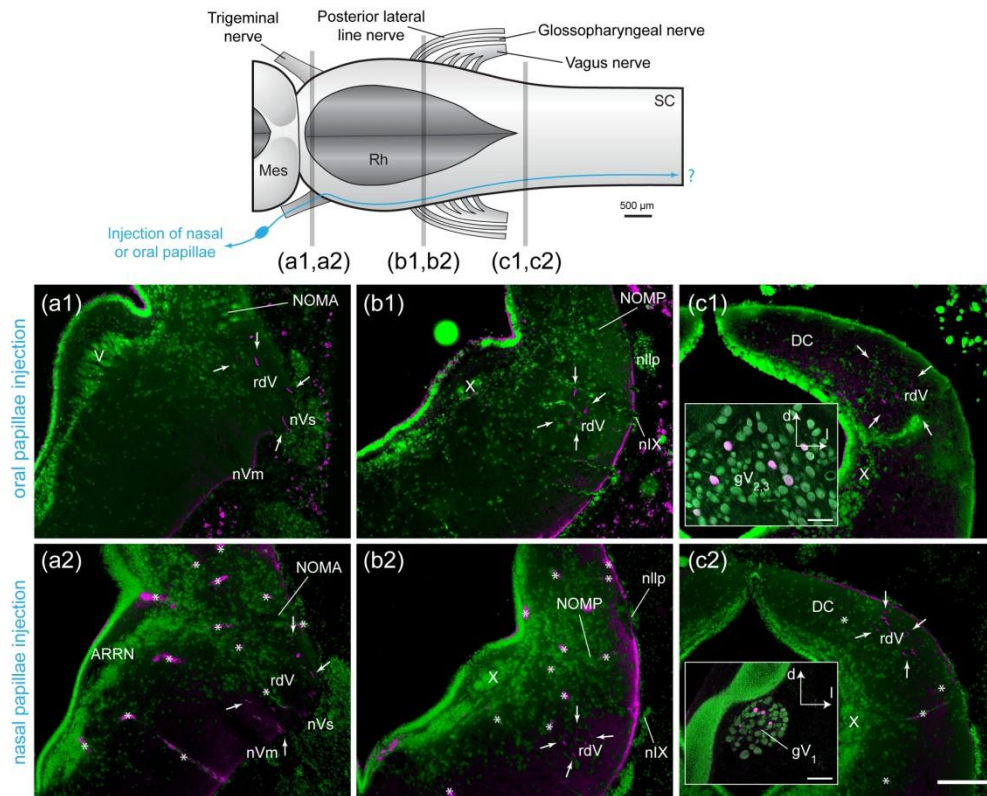
157x203mm (300 x 300 DPI)

Figure 5. Central projections of trigeminal afferents that innervate oral and nasal papillae. The top panel shows a schematic illustration of a dorsal view of the hindbrain showing the extent of the central projections from oral and nasal papillae (blue line). Transverse gray lines represent the levels of the cross sections illustrated in the photomicrographs in the bottom section of the figure. A green fluorescent Nissl stain was used as counterstain. (a1) Fluorescence photomicrograph of a cross section corresponding to level (a1) from the top panel. Fibers labeled from an injection of biocytin in oral papillae (white arrows) enter the brainstem through the trigeminal sensory root (nVs) and then join the descending root of the trigeminal nerve (rdV). (b1) The fibers from the same animal described in (a1) are shown here (between the white arrows) descending in the rdV on a cross section corresponding to level (b1) from the top panel. (c1) The fibers described in (a1) and (b1) are shown here (between the white arrows) descending in the rdV on a cross section corresponding to level (c1) from the top panel. (a2) Fluorescence photomicrograph of a cross section corresponding to level (a2) from the top panel. Fibers labeled from an injection of biocytin in nasal papillae (white arrows) enter the brainstem through the trigeminal sensory root (nVs) and join the descending root of the trigeminal nerve (rdV). Asterisks indicate autofluorescent blood vessels. (b2) The fibers from the same animal described in (a2) are shown here (between the white arrows) descending in the rdV on a cross section corresponding to level (b2) from the top panel. Asterisks indicate autofluorescent blood vessels. (c2) The fibers described in (a2) and (b2) are shown here (between the white arrows) descending in the rdV on a cross section corresponding to level (c2) from the top panel. Asterisks indicate autofluorescent blood vessels. Inset photomicrographs in (c1) and (c2) illustrate trigeminal ganglion cells labeled in the maxillomandibular nerve ganglion (gV2,3) after oral papillae injections (c1) and in the ophthalmicus profundus nerve ganglion (gV1) after nasal papillae injections (c2). ARRN, anterior rhombencephalic reticular nucleus; d, dorsal; DC, dorsal column nucleus; l, lateral; Mes, mesencephalon; nIX, glossopharyngeal nerve; nllp, posterior lateral line nerve; NOMA, anterior octavomotor nucleus; NOMP, posterior octavomotor nucleus; nVm, motor root of the trigeminal nerve; nVs, sensory root of the trigeminal nerve; rdV, descending root of the trigeminal nerve; Rh, rhombencephalon; SC, spinal cord; V, trigeminal motor nucleus; X, vagal motor nucleus. Scale bars over photomicrographs = 200 μm.
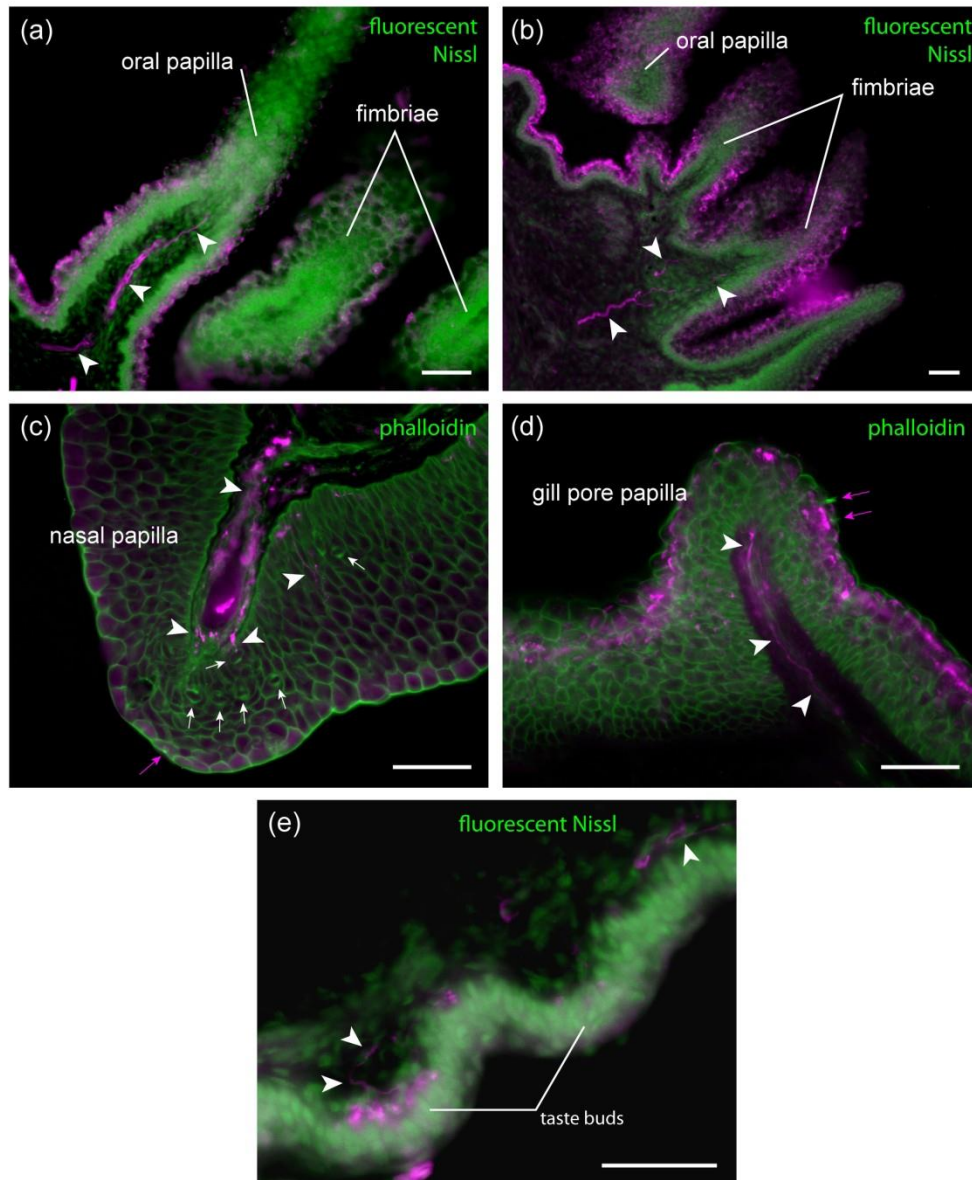
182x146mm (300 x 300 DPI)

Figure 6. Photomicrographs of cross sections of papillae and pharyngeal taste buds showing their innervation. Note that the magenta labeling at the surface of the tissue in (a), (b) and (d) is unspecific autofluorescence. The green channel in (a), (b) and (e) is fluorescent Nissl staining while in (c) and (d), it is phalloidin labeling. (a,b,c) Injecting the trigeminal nerve at its exit from the cranium labeled fibers (arrowheads) innervating the oral (a) and nasal (c) papillae, and the oral fimbriae (b). In (c), many Merkel cells are indicated with white arrows and one out-of-focus SCC is indicated with a magenta arrow. (d) Injecting the glossopharyngeal or vagus nerves at their exit from the cranium labeled fibers (arrowheads) innervating the gill pore papillae. Labeled microvilli from two SCCs are indicated with magenta arrows. (e) Injecting the glossopharyngeal and vagus nerves at their exit from the cranium also labeled fibers (arrowheads) innervating pharyngeal taste buds. Scale bars = 50 μm.
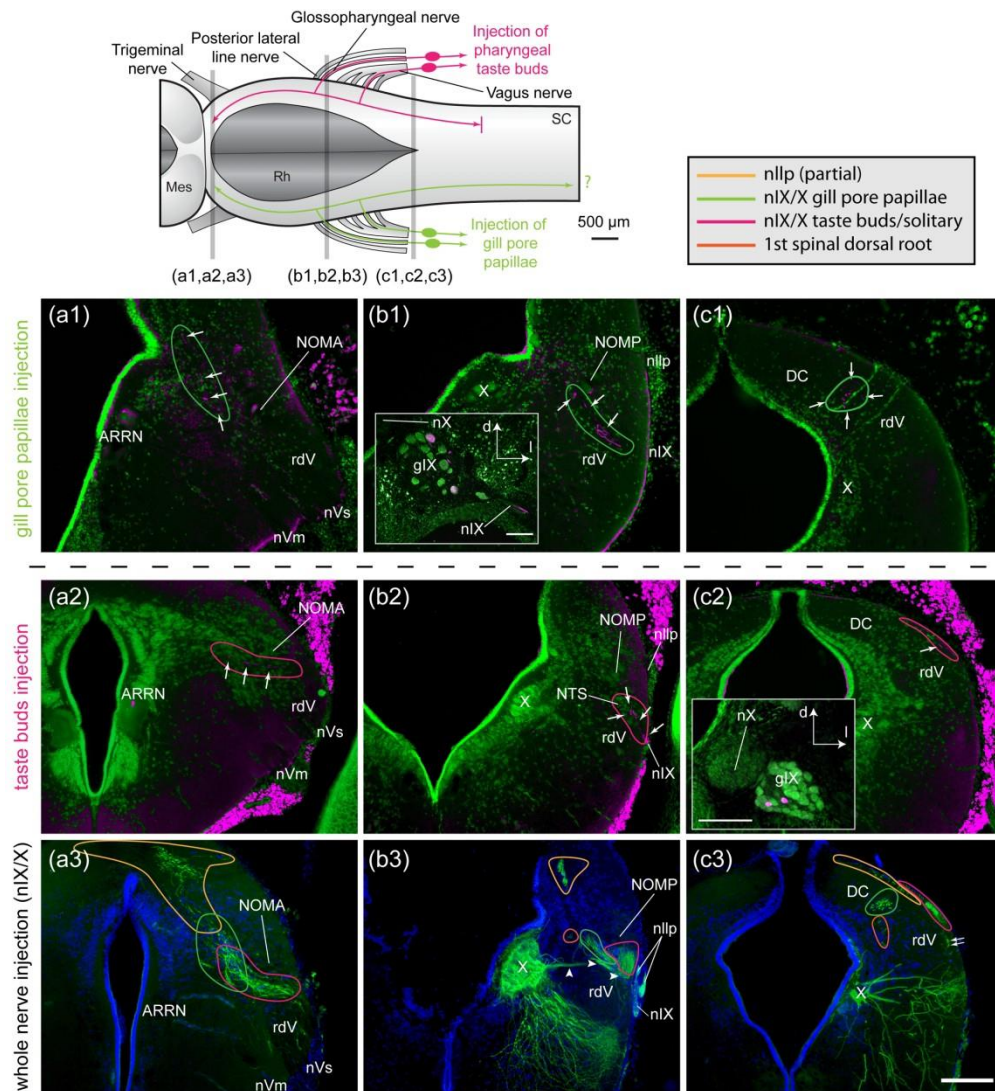
181x218mm (300 x 300 DPI)

Figure 7. Central projections of glossopharyngeal and vagal afferents that innervate gill pore papillae or pharyngeal taste buds. The top panel shows a schematic illustration of a dorsal view of the hindbrain and the extent of the central projections from gill pore papillae (green) and taste buds (magenta). Transverse gray lines represent the levels of the cross sections illustrated in the photomicrographs in the bottom section of the figure. (a1,b1,c1) Photomicrographs of cross sections showing the central distribution of afferents (magenta, indicated with white arrows) labeled after gill pore papillae injection at three different rostro-caudal levels (see top panel for reference). The counterstain is a fluorescent Nissl stain (green). The fibers entered the brainstem through the glossopharyngeal (b1) and vagus nerves. Some fibers ascended to reach isthmic levels (a1) while other fibers descended in the caudal hindbrain (c1) on their way to the spinal cord. The inset in (b1) shows some glossopharyngeal ganglion cells labeled after gill pore papillae injection. (a2,b2,c2) Central distribution of afferents labeled after injection of a few pharyngeal taste buds (magenta, indicated with white arrows) for comparison with gill pore papillae afferents shown in (a1,b1,c1). The counterstain used here is fluorescent Nissl stain (green). Rostro-caudal levels of the cross sections illustrated in photomicrographs in panels (a2,b2,c2) correspond to the levels of panels (a1,b1,c1), respectively. The labeled taste bud afferents entered the brainstem through the glossopharyngeal nerve (b2) and vagus nerve, and many terminated in the nucleus of the solitary tract (NTS, b2), adjacent to the lateral edge of the alar plate. Some fibers ascended to reach isthmic levels (a2), while other fibers descended along the lateral edge of the alar plate (c2) to reach the caudal hindbrain. The inset in (c2)

shows examples of glossopharyngeal ganglion cells labeled after taste bud injection. (a3,b3,c3) Whole nerve labeling showing the central distribution of all afferents from the vagus and glossopharyngeal nerves for comparison with gill pore papillae (a1,b1,c1) and taste bud (a2,b2,c2) afferents. Rostro-caudal levels of the cross sections illustrated in photomicrographs in panels (a3,b3,c3) correspond to the levels of panels (a1,b1,c1) and (a2,b2,c2), respectively (see also top panel for reference). The arrowheads in (b3) indicate axons from motoneurons on their way to exit the brainstem. The white arrows in (c3) indicate a central rootlet of the vagus nerve on its way to join the other taste bud afferents more dorsally located. The counterstain is DAPI, which labels nuclear DNA in blue. For all photomicrographs in the figure, we have delineated each afferent component with a specific color (see color code in the top panel for reference). Note that the whole nerve reference injection of glossopharyngeal and vagus nerves (a3,b3,c3) also labeled sensory fibers entering by the posterior lateral line nerve and the first spinal nerve, as indicat
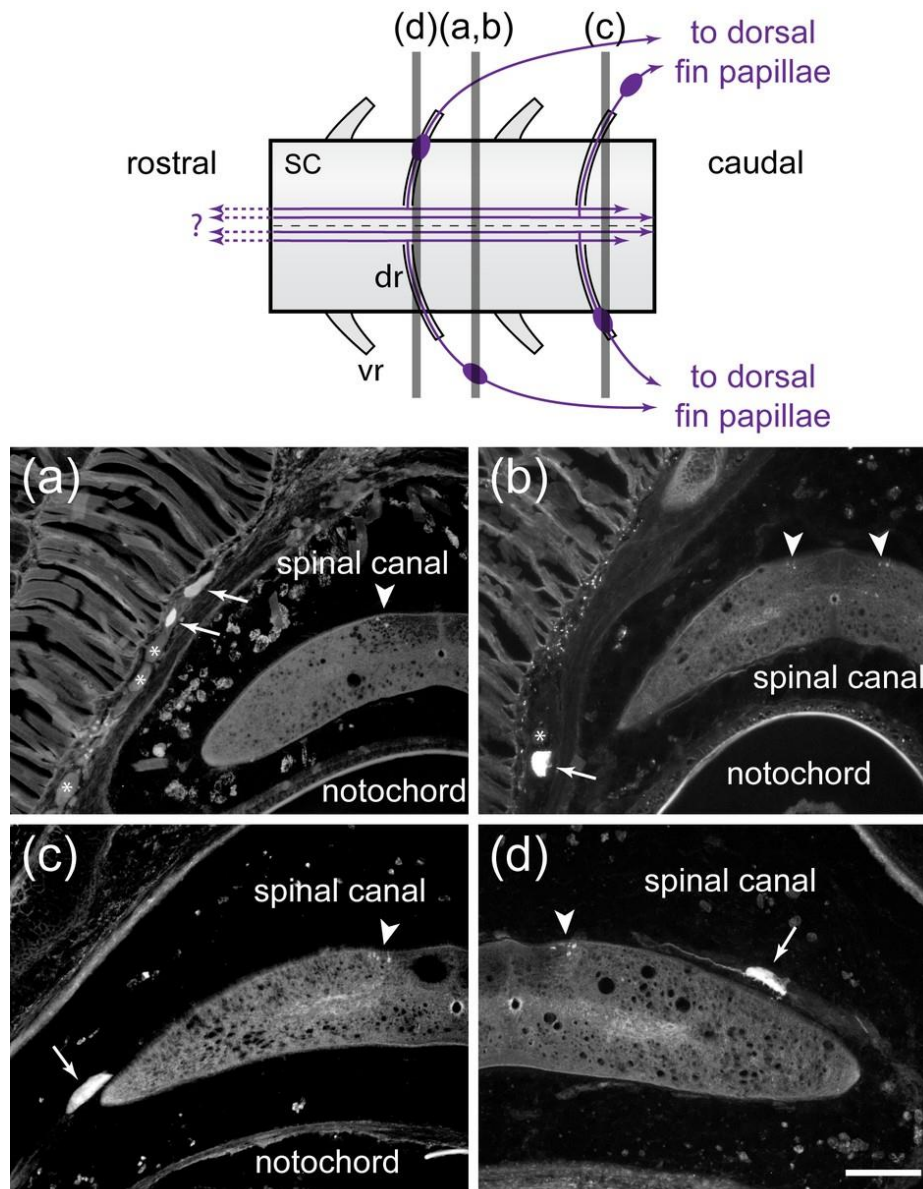
180x196mm (300 x 300 DPI)

Figure 8. Central projections of dorsal root ganglion cells that innervate dorsal fin papillae. The top panel shows a schematic illustration of a dorsal view of the spinal cord showing the extent of the central projections from dorsal fin papillae (purple lines). Transverse gray lines represent the levels of the cross sections illustrated in the photomicrographs in the bottom section of the figure. (a,b,c,d) Photomicrographs of cross sections of the spinal cord and surrounding area at levels corresponding to levels (a) to (d) on the diagram, showing the labeling resulting from dorsal fin papillae injections. (a) Photomicrograph of a cross section of the spinal cord and surrounding area showing two ganglion cells (arrows) located dorsal to the spinal cord, and labeled fibers (arrowhead) in the dorsal columns of the spinal cord. Asterisks were placed over unlabeled ganglion cells. (b) Same as (a) but the labeled ganglion cell (arrow) is located ventral to the spinal cord. Labeled fibers are seen in the dorsal columns (arrowheads) and an asterisk was placed over an unlabeled ganglion cell. (c,d) Same as (a) but the ganglion cells (arrows) are located within the spinal canal. Labeled fibers are found in the dorsal columns (arrowheads). No counterstain was applied. dr, dorsal root; SC, spinal cord; vr, ventral root. Scale bar for all photomicrographs = 200 μm.
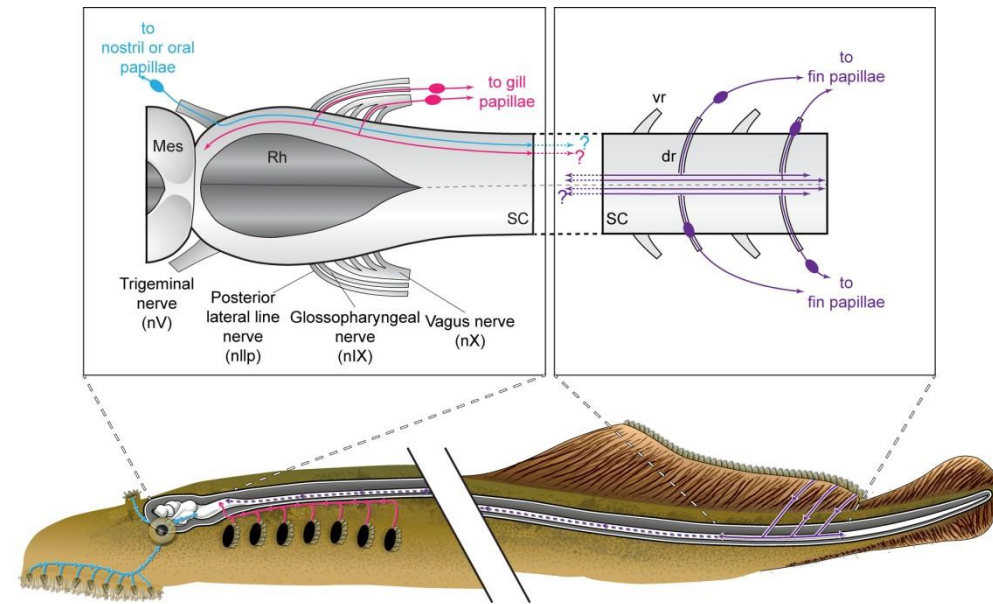
79x103mm (300 x 300 DPI)

Figure 9. The cutaneous papillae innervation and central projections. Top: Schematic illustration of a dorsal view of the hindbrain (left) and caudal spinal cord (right) showing the extent of the central projections from nasal (blue), oral (blue), gill pore (magenta), and fin (purple) papillae. Bottom: Schematic illustration of a lateral view of the head (left) and tail (right) of an adult spawning sea lamprey showing the location of the cutaneous papillae as well as their innervation by cranial and spinal nerves. The nasal and oral papillae are innervated by trigeminal afferents; the gill pore papillae are innervated by glossopharyngeal and vagus afferents; the fin papillae are innervated by spinal dorsal roots afferents.

174x106mm (300 x 300 DPI)

Table 1. Range, mean and standard deviation of the number of cutaneous papillae in *P. marinus*

	Oral disc	Nostril	1st GP	2nd GP	3rd GP	4th GP	5th GP	6th GP	7th GP	Dorsal fin (A)	Dorsal fin (P)
N	11	7	26	26	26	26	26	26	26	3	3
Min	13	13	27	30	29	32	28	29	24	275	515
Max	32	20	43	49	50	52	50	54	42	398	845
Mean	25.6	16.6	36.5	39.7	38.6	41.3	39.4	39.4	34.5	329.3	669.7
S.D.	4.8	2.5	4.9	5.4	8.3	6.9	6.4	7.6	5.4	62.7	166.0

A: anterior; GP: gill pore; N: number of animals; P: posterior.

Table 2. Papillae biometrics

	Oral disc		Nostril		Gill pore		Dorsal fin	
	n=11, 3 animals		n=11, 3 animals		n=19, 4 animals		n=24, 5 animals	
	Length (μm)	Width (μm)	Length (μm)	Width (μm)	Length (μm)	Width (μm)	Length (μm)	Width (μm)
Min	782.2	530.3	136.3	97.0	143.6	58.6	73.7	61.9
Max	1761.4	1087.6	254.5	199.6	341.5	217.1	276.7	157.9
Mean	1300.4	764.9	192.4	159.2	211.7	109.4	171.5	92.3
S.D.	363.3	232.5	37.0	28.4	56.1	39.3	53.7	20.9
Ratio (L/W)	1.7		1.2		1.9		1.9	

Table 3 Responses of gill pore papillae to chemical stimulation

	1	2	3	4	5	6	7	8	9	10	11	12	13	R	N	%
Trout water	red	red	red	red	red			red	red	red	red	red	red	11	13	84.6
Glycine	red	red	red	red	red		red	red					nt	7	12	58.3
Proline	red	red	red				red	red	red	red			nt	7	12	58.3
Taurocholic Acid	red	red		red	red	red								5	13	38.5
Serine	red			red	blue	blue							nt	4	12	33.3
Sialic Acid	red	red	red	nt			nt					nt		3	10	30.0
Glutamate	red	red				blue							nt	3	12	25.0
Arginine						blue							nt	1	12	8.3
Histidine							red						nt	1	12	8.3
Ringer's							red							1	13	7.7
3kPZS	nt		nt		nt	nt			nt	nt	nt	nt	nt	0	4	0.0
3kACA	nt		nt		nt	nt			nt	nt	nt	nt	nt	0	4	0.0

Cross-table showing the individual responses of gill pore papillae from 13 animals to 12 different compounds. All compounds were tested at 10^{-3} M except for the pheromones (3kPZS, 3kACA; 10^{-5} M) and the trout water (unknown concentration). Colored squares indicate significant excitatory (red) or inhibitory (blue) responses. Grey squares indicate the absence of significant responses. nt: not tested; N: number of animals tested; R: number of animals displaying significant responses;%: relative effectiveness (R/N*100).